energies

MDPI

Review

Recent Trends in the Production, Combustion and Modeling of Furan-Based Fuels

Mazen A. Eldeeb [1,*] and Benjamin Akih-Kumgeh [2]

[1] Department of Mechanical Engineering, California State University, Fresno, Fresno, CA 93740, USA
[2] Department of Mechanical and Aerospace Engineering, Syracuse University, Syracuse, NY 13244, USA; bakihkum@syr.edu
* Correspondence: meldeeb@csufresno.edu; Tel.: +1-559-278-1044

Received: 12 January 2018; Accepted: 22 February 2018; Published: 27 February 2018

Abstract: There is growing interest in the use of furans, a class of alternative fuels derived from biomass, as transportation fuels. This paper reviews recent progress in the characterization of its combustion properties. It reviews their production processes, theoretical kinetic explorations and fundamental combustion properties. The theoretical efforts are focused on the mechanistic pathways for furan decomposition and oxidation, as well as the development of detailed chemical kinetic models. The experiments reviewed are mostly concerned with the temporal evolutions of homogeneous reactors and the propagation of laminar flames. The main thrust in homogeneous reactors is to determine global chemical time scales such as ignition delay times. Some studies have adopted a comparative approach to bring out reactivity differences. Chemical kinetic models with varying degrees of predictive success have been established. Experiments have revealed the relative behavior of their combustion. The growing body of literature in this area of combustion chemistry of alternative fuels shows a great potential for these fuels in terms of sustainable production and engine performance. However, these studies raise further questions regarding the chemical interactions of furans with other hydrocarbons. There are also open questions about the toxicity of the byproducts of combustion.

Keywords: furans; biofuels; second generation biofuel; production methods; combustion; ignition characterization; laminar burning velocity; engine performance; chemical kinetic modeling

1. Introduction

Fossil fuels are considered the principal source of energy in the world, accounting for nearly 82% of the global energy consumption [1], but 57% of greenhouse gas emissions are fossil-fuel related [2]. One of the main challenges for society is the development of affordable and environmentally-friendly energy sources to replace fossil fuels in the future. The use of biofuels is a promising alternative, especially in the transportation sector, which accounts for 21% of the global energy consumption [1]. Biofuels are also of interest because of their ability to substitute fossil fuels without major engine modifications. In addition, their greenhouse gas emissions are significantly lower than those of fossil fuels, since the emitted CO_2 from combustion is recycled in agricultural activities.

In transportation systems, spark ignition (SI) engines are the most dominant technology. Among the biofuels used in SI engines, furans have emerged as promising alternative fuels. They can be produced from sugars originating from second-generation biomass [3–7], and they also possess favorable combustion properties that could promote their use in SI engines. For instance, the furan 2,5-dimethylfuran (2,5-DMF) has a higher energy density of 30 MJ/L and better resistance to undesired ignition with a research octane number (RON) of 119 compared to ethanol, the most commonly-used biofuel in SI engines with a RON of 110. As a result of these features, furans might be useful for

modifying the combustion behavior of conventional fuels toward higher efficiency engine operation and lower emissions.

Recent progress has been made in characterizing and modeling the combustion properties of furans. Ignition studies of these fuels have focused on individual cases, as well as systematic comparative studies to establish fuel structure-reactivity trends. These established trends are aimed at improving emerging chemical kinetic models [8–11]. Other studies focus on the exploration of blending effects on the ignition of furans and gasoline mixtures.

This review looks at progress in theoretical and experimental efforts geared toward furan combustion fundamentals. Recent studies show that furans are promising candidates for use in SI engines without significant modifications. Various engine studies show that the combustion of furans exhibits better knock resistance and lower emissions of NO_x, hydrocarbons (HC) and particulate matter (PM) than conventional gasoline and well-established biofuels, such as bio-ethanol [12–20]. Auto ignition of furans has been also investigated. Furan, as well as the alkylated furans 2,5-dimethylfuran (2,5-DMF) and 2-methylfuran (2-MF) have been the focus of individual and comparative ignition studies, as well as some modeling studies [8–11,21–25]. The saturated furans, tetrahydrofurans, are equally promising as fuel additives or pure fuels. Despite the fact that the saturated furans are not as extensively studied as alkyl furans, there is an increasing interest in computational and experimental characterizations of their combustion [22,26–29].

Despite the increasing number of ignition studies of furans, a number of gaps and open questions have been identified. One problem is that only a few studies focus on structure-activity trends. These limited studies raise further questions regarding the chemical interactions of furans with other hydrocarbons, posing a challenge to model reduction and raising questions about the toxicity of the byproducts of combustion. With respect to chemical kinetic modeling, ignition delay time and laminar burning velocity predictions of existing models of furans need further improvement, guided by an extended experimental database of various combustion properties.

The review is divided into four main sections. The first is a classification of different types of furans and a review of the most widely-used methods of their production. The second will focus on theoretical and experimental investigations of furans' decomposition and oxidation. These include quantum chemical kinetic calculations, experimental studies of the pyrolysis of furans in flow reactors and detailed chemical kinetic modeling. The third section will be dedicated to the characterization of furan combustion properties through engine studies, characterization of individual and comparative auto-ignition behavior, as well as studies of laminar burning velocities. The fourth section will expand on modeling efforts, by reviewing model validation studies. Conclusions and the future outlook are given.

2. Classification and Production Methods of Furans

The combustion performance of furans needs to be appraised alongside the evaluation of the means of their production from biomass. The fact that the transportation sector is geographically and technologically diverse and the fact that furanic compounds will most likely be used in blends or as additives rather than single fuel components complicate the estimation of the practical production scale. However, it is necessary that the biomass feedstocks do not compete with other biomass usages, which makes lignocellulose the raw material of choice in this case, as it does not compete with food production.

This section presents a classification of furanic fuels based on chemical structure. Moreover, it reviews the various production methods from biomass feedstock. A representative bio processing plant is shown in Figure 1. The process starts with the drying of biomass to prepare it to subsequent gasification, in which the carbon-based biomass is oxidized at high temperatures of 1073–1473 K. The gasification process produces a combustible mixture of CO_2 and hydrogen. This mixture is cleaned up and fermented. Then, it can be converted into biofuels, including furans, through distillation and dehydration. Furanic biofuels can be categorized under two main groups in this text. The first is furan

and substituted furans, while the second is tetrahydrofuran and alkyl tetrahydrofurans. These two groups call for different production processes.

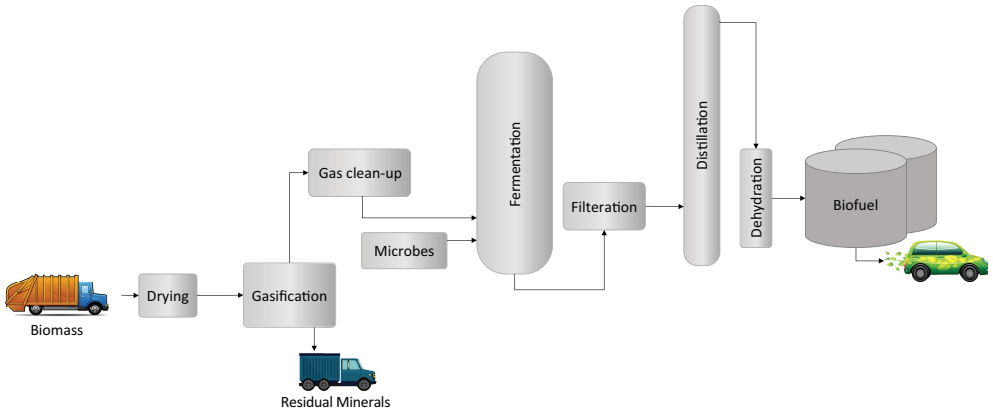

Figure 1. Sketch of a representative bio processing plant (inspired by Aylott [30]).

2.1. Furan and Substituted Furans

Furan and substituted furans are mostly obtained from the platform chemicals called furfural and 5-hydroxymethyl-2-furaldehyde (HMF) (see Figure 2). The processes involve bond-breaking and bond-formation through hydrogenation and dehydration reactions. The synthesis also involves important reactions such as deoxydehydrogenation, hydrogenolysis, decarboxylation and decarbonylation [31]. The chemical structures of furan and some substituted furans are shown in Figure 2. The focus of this subsection will be on the most promising substituted furanic biofuels, namely 2-methylfuran (2-MF) and 2,5-dimethylfuran (2,5-DMF) [32,33]. Table 1 shows some of the thermophysical properties of 2-MF and 2,5-DMF.

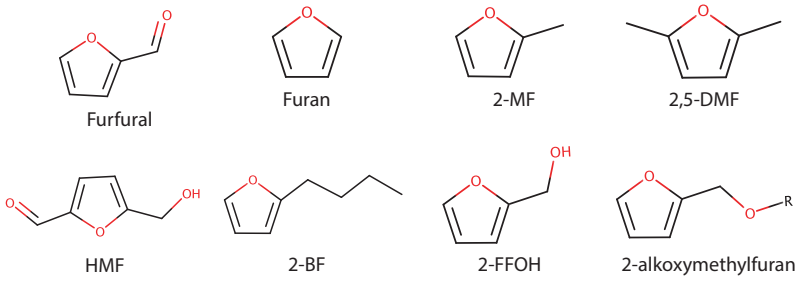

Figure 2. Chemical structures of starting platforms and resulting fuels for furan and substituted furans. HMF, 5-hydroxymethyl-2-furaldehyde; 2-BF, 2-butylfuran; 2-MF, 2-methylfuran; 2-FFOH, 2-furfuryl alcohol; 2,5-DMF, 2,5-dimethylfuran.

Table 1. Thermophysical properties of the most promising furan-based biofuels [31,34,35]. 2-MTHF, 2-methyltetrahydrofuran; RON, research octane number.

Property \ Compound	2-MF	2,5-DMF	THF	2-MTHF
Boiling point (K)	336	365	339	353.2
Density (g/cm^3)	0.91	0.89	0.8892	0.854
Lower heating value (MJ/kg)	31.2	33.8	34.6	32.8
RON	103	119	–	86

2.1.1. 2-Methylfuran

The next simplest furan is 2-MF, which is a flammable liquid, insoluble in water. It naturally exists in myrtle and Dutch lavender plants [31]. 2-MF is a promising liquid fuel candidate as shown by a number of studies, including an extensive road test which lasted over 90,000 km with satisfactory outcomes [36,37]. The thermophysical properties of 2-MF indicate that 2-MF is a promising additive to fossil fuels [38]. Generally, 2-MF can be synthesized through the hydrogenation of furfural via an intermediate compound, 2-furfuryl alcohol (2-FFOH). High temperatures up to 553 K and high pressure of H_2 are necessary for this reaction scheme, which leads to the production of 2-MF along with 2-pentanone, 2-pentanol and 2-methyltetrahydrofuran (2-MTHF) [31].

Studies of 2-MF production from furfural emerged around the 1940s [39]. Twenty-three different catalysts and catalyst carriers were investigated for hydrogenation of furfural at vapor-phase to 2-MF at 1 atm and a temperature range of 473–503 K. The study showed that the most successful catalyst was copper chromite dispersed on activated charcoal, with 90–95% yields of 2-MF obtained in one pass of furfural at a rate of 20–30 g/h. Further, a method to produce 2-MF in the liquid phase was proposed by Sun et al. [40] through the hydrogenolysis of furfural using a polymer-supported Pd(11) catalyst. The authors reported a 100% yield within one hour at a temperature of 291 K and a hydrogen pressure of 0.1 MPa. Another study by Rao et al. [41] investigated the hydrogenation of furfural to 2-MF over copper catalysts dispersed on activated carbon, diamond and graphitized fibers. While the hydrogenation of the C=O bond to form 2-MF only took place at a temperature range of 473–573 K, the most active catalyst was identified at 573 K, which was the Cu/activated carbon catalyst. The vapor-phase hydrogenation of furfural studied by Zheng et al. [42] and discussed earlier was also used for the production of 2-MF. The results revealed that the use of C_1 catalyst in the hydrogenation of furfural achieved better 2-MF yields than C_2 catalyst, with up to 87.0% yield at 523 K. The same behavior was observed in the case of the conversion of furfuryl alcohol to 2-MF. Later, a new environmentally-friendly Cu–Zn–Ca/γ-Al_2O_3 catalyst was used for furfural hydrogenation at vapor-phase to 2-MF in a study by Li and Li [43]. The results showed that a 2-MF selectivity exceeding 99% and a yield of 97% were achieved at a temperature of 508 K. Moreover, the above-mentioned study of Sitthisa et al. [44] also investigated 2-MF formation through the conversion of furfural in hydrogen over SiO_2-supported nickel and Ni-Fe bimetallic catalysts. Using the Ni catalyst, furfuryl alcohol was produced through hydrogenation, which further produced 2-MF through C–O hydrogenolysis. The use of Fe–Ni catalysts significantly increased the yield of 2-MF since the addition of Fe inhibited the decarbonylation of Ni and favored the low-temperature C=O hydrogenation and the high-temperature C–O hydrogenolysis. Later on, the conversion of furfural to 2-MF in n-butanol catalyzed by carbon supported ruthenium (Ru/C) was investigated in a study by Zhang et al. [45]. A yield of up to 61.9 mol% was achieved. Another method of 2-MF production was presented by Nilges and Schröder [46], based on the electrochemical conversion of furfural to 2-MF at room temperature. The authors claimed that the selectivity of 2-MF achieved in their study was unprecedented. One of the most important results was that 100% conversion of furfural to 2-MF was achieved using copper electrodes. Moreover, an 80% selectivity to 2-MF was observed, which is an order of magnitude higher than previously reported electrochemical processes. Focusing on the use of Cr-free copper catalysts for the conversion of furfural to 2-MF, Dong et al. [47] investigated the preparation and utilization of three copper catalysts (Cu/Al_2O_3, Cu/SiO_2 and Cu/ZnO). It was shown that the Cu/SiO_2 catalyst achieved the highest 2-MF yield of 89.5%, due to synergistic effects of Cu and weak acid sites. The high dispersion of Cu particles in the catalyst contributed to its activity. The same research group of Dong et al. [47] presented another study that used an AE–Cu/SiO_2 catalyst prepared by ammonia evaporation (AE) for the synthesis of 2-MF [48]. The 2-MF yield was shown to be 95.5%, due to the effects of surface species and acid sites. The catalyst production by ammonia evaporation led to the formation of several Cu nanoparticles and acid sites, which enhanced the catalyst activity and selectivity. Moreover, the AE–Cu/SiO_2 catalyst showed improved stability. Compared

to a conventional CP–Cu/SiO_2 catalyst, the catalyst showed a significantly improved yield and an extended lifetime.

Other methods of 2-MF production have also been investigated, combining furfural and other platform chemicals [49–51]. A novel process of 2-MF formation that coupled furfural hydrogenation and 1,4-butanediol dehydrogenation over the same Cu-based catalyst was explored by Zhu et al. [49]. The coupled reaction led to a significant increase in 2-MF yield, compared to those in the individual reactions, with 2-MF yields up to 88.6% at a temperature of 485 K. Moreover, another study by Zheng et al. [50] demonstrated a new 2-MF production process that combined cyclohexanol dehydrogenation and furfural hydrogenation over a Cu–Zn–Al catalyst. The results showed that the new process was more energy efficient and environmentally benign. The results showed that furfural was almost completely converted over a temperature range of 493–573 K using the Cu–Zn–Al catalyst. However, the operation temperature affected the selectivity of 2-MF, with the maximum selectivity being 87.0% at 523 K. In a more recent study by Zheng et al. [51], a co-precipitation method was used to prepare a number of Cu–Mn–Si catalysts for the purpose of producing 2-MF by combining cyclohexanol dehydrogenation and furfural hydrogenation. The results showed that manganese had a positive effect on the activity of cyclohexanol dehydrogenation and furfural hydrogenation. It also increased the selectivity of 2-MF up to around 91%. The study showed that a Cu–Mn–Si catalyst with a molar ratio of Cu:Mn:Si = 1:1.12:1.13 provided the highest activity, selectivity and stability under reaction conditions.

Methods that utilize sources other than furfural were investigated [52–54]. The furan production method from food investigated by Limacher et al. [52] and discussed earlier was also used for the production of 2-MF. The results showed modest yields of 2-MF during the synthesis from sugars in aqueous systems (<25 μmol/mol). However, the yields of 2-MF in Maillard reactions systems were relatively higher under roasting conditions (i.e., 160–260 μmol/mol). Moreover, higher yields of 2-MF could by achieved at pH levels of 7. A selective method to produce 2-MF from furfuryl alcohol at room temperature was investigated by Iqbal et al. [53] under very low H_2 pressures using Pd catalysts supported by very small particles (<2 nm). The results showed that the main pathway was the hydrogenated deoxygenation of O–H in furfuryl alcohol, while the C=C reduction was suppressed. The only byproduct observed was tetrahydrofurfuryl alcohol (<6%). Recently, the synthesis of 2-MF from xylose in a continuous fixed-bed reactor was presented [54]. The process utilized a combined catalyst consisting of Hβ zeolite and Cu/ZnO/Al_2O_3 in a solvent of γ-butyrolactone (GBL)/water. The Hβ zeolite and GBL were shown to facilitate the dehydration of xylose and significantly improve the yield. The results showed that altering the hydrogenation temperature for furfural affected the 2-MF yield. The highest yield achieved in this process for 2-MF was 86.8% at a temperature of 463 K.

The production of 2-MF has also been explored computationally. An example of this is the work by Vorotnikov et al. [55] mentioned earlier. The results showed that the typical pathway for the 2-MF formation from furfuryl alcohol was hydrogen-assisted dehydration, which had an activation barrier 4.612 kcal/mol lower than dehydroxylation. Alternatively, 2-MF can also be produced according to the study through dehydrogenation to a methoxy intermediate, followed by deoxygenation.

Thus, a number of catalytic 2-MF production methods have been explored, some are characterized by high yields. Some mechanistic explorations have been offered for the observed trends.

2.1.2. 2,5-Dimethylfuran

2,5-DMF is a colorless liquid that is insoluble in water. This bio-derived compound has interesting combustion properties that are comparable with gasoline and are superior to bioethanol, especially with regards to energy density and engine performance [7,56–60]. Moreover, it was found that the 2,5-DMF exhibits antiwear and antifriction properties that exceed those for commercial gasoline [61]. These properties have inspired numerous research groups to investigate sustainable methods of 2,5-DMF production, with the aim of using it as a liquid transportation fuel.

The lead effort in 2,5-DMF production from biomass was that of Román-Leshkov et al. [3], who presented a catalytic approach for 2,5-DMF synthesis from fructose, which can be produced directly from biomass or through glucose isomerization. As shown in Figure 3, this catalytic strategy starts with the selective fructose dehydration in a biphasic reactor, leading to the formation of 5-hydroxymethylfurfural (HMF). This is followed by the evaporation of water and hydrochloric acid from the liquid solvent containing HMF, resulting in the precipitation of NaCl. After that, HMF undergoes hydrogenolysis over a CuRu catalyst to produce 2,5-DMF. Finally, the 2,5-DMF is separated from the solvent and intermediates. The process resulted in 2,5-DMF yields of 71% in liquid-phase hydrogenolysis and 76–79% in vapor-phase hydrogenolysis. The authors suggested that while using glucose instead of fructose would improve wide-scale production of 2,5-DMF because of the higher availability of glucose, using fructose provides greater selectivity of 2,5-DMF. This finding was later confirmed by Paine et al. [62], who reported that the fructose/glucose 2,5-DMF formation ratio was found to be about 1.77.

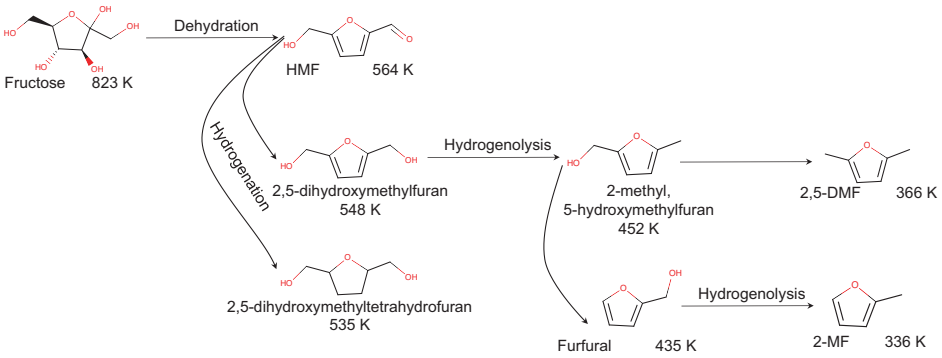

Figure 3. A schematic for the production of 2,5-DMF, 2-MF and other biofuels from fructose (adapted from Román-Leshkov et al. [3]).

The work of Román-Leshkov and co-workers has motivated other researchers to investigate alternative production methods of 2,5-DMF [5,63–65]. For instance, Binder and Raines [63] presented a two-reaction process to produce 2,5-DMF from lignocellulosic biomass. The first step was the formation of HMF from corn stover in *N*,*N*-dimethylacetamide (DMA) dissolved in lithium chloride (LiCl). Then, the chloride ions were separated from the crude HMF by ion-exclusion chromatography. The crude HMF was finally subjected to hydrogenolysis in 1-butanol with a carbon-supported CuRu catalyst. The process achieved a 49% molar yield of 2,5-DMF. Later on, another two-step process to convert glucose to 2,5-DMF was described by Chidambaram and Bell [5,66]. The first step was glucose dehydration to HMF dissolved in ionic liquids. Next, Pd/C was used for the hydrogenation of HMF to 2,5-DMF, with yields of about 16%. The authors attributed the reduced 2,5-DMF yield to the reduced time of reaction and temperature and the low H_2 solubility in ionic liquids. Further, a study by Thananatthanachon and Rauchfuss [64] used formic acid as a renewable H_2 carrier to perform "one-pot" synthesis of 2,5-DMF from fructose. The study indicated that formic acid can be used as a catalyst to dehydrate fructose to HMF, which serves as a hydrogen source and a deoxygenating agent, motivating the attempt to combine some of the 2,5-DMF production steps. The study showed that an excellent yield of 2,5-DMF exceeding 95% could be obtained by heating HMF in refluxing THF with formic acid, sulfuric acid and Pd/C. In another study by Luijkx et al. [65], the synthesis of 2,5-DMF was performed by subjecting HMF to hydrogenolysis over Pd catalysts in 1-propanol. The main intermediate in the process was 5-hydroxymethyl-2-(propyloxymethyl)furan. Using 2-propanol as a solvent led to ether formation, while using 1,4-dioxane led to the formation of 2,5-bis(hydroxymethyl)furan [4].

The use of Ru/C catalysts for the hydrogenation of HMF to 2,5-DMF was extensively investigated in a number of studies [36,45,67–70] under various temperature ranges and using difference hydrogen

sources. These studies demonstrated different yields and conversion rates. The highest 2,5-DMF yield was reported by Hu et al. [70], which reached 94.7% with total HMF conversion at a reaction temperature of 473 K for 2 h. The results showed that further temperature increase up to 533 K did not affect 2,5-DMF yields [45].

Other catalytic conversion studies of HMF to 2,5-DMF were performed, using catalysts such as nickel-tungsten carbide [71], Lewis-acidic Zn^{II} and Pd/C [72], PdAu/C [73], Ru/Co_3O_4 [74], ruthenium-containing hydrotalcite (HT) [75], Ru–Sn/ZnO [76], Ni/Co_3O_4 [77], palladium-cesium dodeca-tungstophosphoric acid on K-10 clay [78] and graphene oxides-supported platinum (Pt/rGO) [79]. Most recently, carbon-coated Cu–Co bimetallic nanoparticles were also used, exhibiting the best performance [80]. Using a carbon-coated Cu–Co catalyst, an excellent 2,5-DMF yield of 99.4% was achieved. The authors suggested that the entrapment of bimetallic nanoparticles by carbon shells contributed to this behavior, as the nanoparticles were protected from oxidation and deactivation.

Another study by Dutta and Mascal [81] demonstrated a new approach to produce 2,5-DMF by the conversion of biomass-derived 5-(chloromethyl)furfural (CMF) into intermediates that can be readily hydrogenated under very mild conditions, leading to renewable pathways to 2,5-DMF that avoid HMF as an intermediate. This work is motivated by the challenging HMF accessibility from lignocellulosic biomass. The study reports a 65% yield from raw biomass to 2,5-DMF, compared to corresponding yields from cellulose and sucrose of 68 and 73%, respectively.

Electrochemical methods for 2,5-DMF have also been explored. In a study by Nilges and Schröder [46], an electrochemical process for the conversion of HMF to 2,5-DMF is presented for the first time. The results show that the highest yields were achieved at Cu electrodes. The highest 2,5-DMF selectivity (35.6%) was obtained in a sulfuric acid solution in a mixture of water and ethanol. The process consists of a series of steps of 2-electron/2-proton reduction, in which six electrons and six protons are required for the transformation of HMF to 2,5-DMF.

Few studies have focused on the economics of furan production. A unique perspective about the economics of mass-production of 2,5-DMF was presented in a study by Kazi et al. [82], which investigated the economics of 2,5-DMF from fructose in a three-train catalytic plug flow tubular reactor. The analysis revealed that the minimum profitable selling price (MSP) was estimated at $7.63/gal. A sensitivity analysis was performed to investigate the possible determinants of the MSP of 2,5-DMF and their impact on the selling price. It was found that the yield of 2,5-DMF from fructose is the main determinant of the MSP, where a 20% increase in the yield leads to 16.7% reduction in the MSP. The fructose price affects the MSP so that a 20% decrease in the fructose cost reduces the MSP by 9.3%. Other important determinants are equipment cost, Cu–Ru/C catalyst cost and levulinic acid cost.

From the above review, we see that a number of 2,5-DMF production methods have been investigated. These include catalytic and electrochemical methods of converting HMF to 2,5-DMF. Some insights into the economics of 2,5-DMF were demonstrated, but the economic studies are limited.

2.2. Tetrahydrofuran and Alkyl Tetrahydrofurans

The second group of furans to be discussed in this section is tetrahydrofuran and alkyl tetrahydrofurans. This group of furanic compounds is mostly obtained from the platform chemicals succinic acid, levulinic acid and itaconic acid [31] (see Figure 4). The chemical structures of tetrahydrofuran and some alkyl tetrahydrofurans are presented in Figure 4. The focus of this subsection will be on tetrahydrofuran (THF) and 2-MTHF, which have received greater attention for combustion system applications. The thermophysical properties of these biofuels are shown in Table 1.

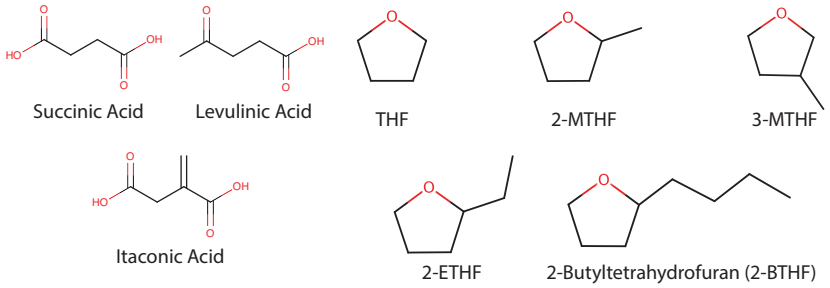

Figure 4. Chemical structures of starting platforms and resulting fuels for THF and select alkyl THFs. 2-ETHF, 2-ethyltetrahydrofuran.

2.2.1. Tetrahydrofuran

THF is a flammable, colorless liquid that is miscible with water. THF is mainly used for the production of poly(tetramethylene ether) glycol as a chemical solvent [31,83]. It is also being considered as a biofuel candidate.

Efforts on the production of THF have been reported since the 1940s. In a study by Wilson [84], tetrahydrofurfuryl alcohol vapor was passed over a Ni or Ni-containing catalyst above 473 K, which led to the elimination of the side chain of the alcohol as CO and H_2 to produce a liquid product in which THF was major constituent (61.8 wt%), with the THF yield reaching 96% [42,84]. A similar approach for eliminating the side chain of tetrahydrofurfuryl alcohol to produce THF was employed by Bagnall et al. [85] using catalysts with various nickel content between 20 and 100%. The results revealed that the highest THF yield was 85%, achieved with a catalyst containing 44% nickel. The study indicated that pure Ni had much lower catalytic effectiveness, while pure Cu was inactive as a catalyst. The results attributed the catalytic activity and the high THF yield to the almost total filling of the d-levels of Ni atom, which occurs at about 44% Ni–Cu, leading to a more strongly-suppressed destructive hydrogenative side reactions [42,85].

The production of THF from succinic acid was investigated in a number of studies [86–89]. A process for the continuous production of THF was presented by Kanetaka et al. [86], through the direct maleic anhydride hydrogenation to succinic acid, which is further hydrogenated to THF. The study shows that the process provided a high selectivity to THF, up to 90%, and full conversion of maleic anhydride per-pass. Succinic acid hydrogenation in aqueous ethanol under mild pressures and temperatures was investigated for the first time by Luque et al. [87], using stable supported metal nanoparticles of Pt, Pd, Rh and Ru on Starbon®-300 (mesoporous carbon) to produce THF. The selectivity of THF was 60% at 24 h, which further increased to 82% after 34 h. In a study by Minh et al. [88], the production of THF through the hydrogenation of succinic acid was presented. THF was produced in this process as a by-product, while the major product was 1,4-butanediol. Using a 2 wt% Ru/C catalyst led to the complete conversion of succinic acid over a reaction period of 35 h. Succinic acid was converted to γ-butyrolactone and then further converted to THF. The conversion was not completed when a 2 wt% Pd/C catalyst was used for 50 h. Furthermore, a rhenium catalyst supported by mesoporous carbon (MC) treated with different H_2SO_4 concentrations (Re/MC–*X*) was employed for the hydrogenation of succinic acid at liquid-phase to THF in a study by Hong et al. [89] at 513 K and H_2 pressure of 80 bar. The results showed that using an H_2SO_4 concentration of 0.4 M in the catalyst led to total succinic acid conversion and a maximum THF yield of 38.3%.

THF can also be produced by the ring-hydrogenation of furan and ethylfurfuryl [37,90,91]. The selective hydrogenation of furan into THF was performed in a study by Godawa et al. [92] at a pressure of 20 bar and a low temperature of 373 K by use of a catalyst containing 5% Pd microporously supported on carbon B. The conversion rate reported by the study was 150 mL of THF per gram of catalyst per hour, which was achieved in the absence of furfural or CO.

The production of THF from corn stalks, a form of agricultural waste rich in pentosans, was investigated by Godawa et al. [93]. The authors used charcoal-supported catalysts in the furan hydrogenation reaction under constant H_2 pressure, while no solvent was used.

Furfural is also one of the key sources for THF, which is catalytically decarbonylized to furan, and then, the hydrogenation of furan gives THF [94,95]. In a study by Zhang et al. [96], the catalytic performance of K-doped Pd/Al_2O_3 catalysts was investigated during the decarbonylation of furfural to THF over a temperature range of 453–533 K and atmospheric pressure. The results revealed that doping the $Pd–K/Al_2O_3$ catalyst doped with K_2CO_3 with an 8 wt % K-loading achieved total furfural conversion and a maximum THF and furan yields in the decarbonylation reaction.

However, Yan and coworkers [91] highlighted one of the biggest challenges facing the production of THF from furfural, which is the by-production of coke. This poses a problem because it reduces the total possible THF yields and also reduces the catalytic activity for catalysts such as Ni/zeolite. The study proposed addition of an H_2 donor as a possible method of limiting the yield of coke.

From the foregoing review, we see that a number of THF production methods from various platform chemicals have been proposed and investigated, some offering high yields and selectivity.

2.2.2. 2-Methyltetrahydrofuran

2-MTHF has limited miscibility with water and is easy to degrade in sunlight and air, which makes it environmentally promising in various applications [31]. 2-MTHF can be readily used in blends with gasoline without major engine modifications. Although the lower heating value of 2-MTHF is lower that that of gasoline, the higher density of 2-MTHF compensates for the heating value difference, and therefore, 2-MTHF exhibits similar engine performance to gasoline [97], based on liquid volume.

The reported efforts regarding the synthesis of 2-MTHF go as far back as the 1940s, with the study of Christian et al. [98] who demonstrated the use of a Cu–Cr catalyst for the hydrogenation of levulinic acid at 573 K and 200 atm of H_2, with a low amount of 2-MTHF (4.5% yield) as a by-product. A similar yield was achieved by Yan et al. [99], who used a noble-free Cu–Fe catalyst for the hydrogenation of levulinic acid, achieving a 2-MTHF yield of 3.5%. Even lower yields of 2-MTHF were achieved using Cu-based Fe-free catalysts [47]. The most common pathway for 2-MTHF production is the catalytic hydrogenation of levulinic acid, which is reduced to 4-hydroxypentanoic acid, and then dehydrated to γ-valerolactone (GVL) [94,100,101]. This is followed by the hydrogenation of GVL to 1,4-pentanediol, which is finally dehydrated to 2-MTHF [94]. In a study by Bozell et al. [100], a single-stage catalytic hydrogenation of levulinic acid was performed for the synthesis of 2-MTHF, resulting in >80% molar yield. Furthermore, Mehdi et al. [101] used Ru-based catalysts for the hydrogenation of both levulinic acid and furfural, via γ-valerolactone and 2-MF, respectively. 2-MTHF yields reached 72% at 473 K. A similar approach was employed by Du et al. [102], who employed a copper-zirconia catalyst for the hydrogenation of GVL to 2-MTHF in reasonable yields. Other studies investigated the production of 2-MTHF from levulinic acid [103,104]. Upare et al. [103] used Cu/Si nanocomposite catalysts for the direct levulinic acid hydrocyclization at vapor-phase to 2-MTHF, under moderate H_2 pressures. The highest selectivity of 2-MTHF was 89%, which was achieved using nickel-promoted Cu/Si catalyst with a 72 wt % copper loading. Furthermore, Geilen et al. [104] used a catalyst that combines both acidic and ionic features to produce 2-MTHF from levulinic acid. The authors used the acidic ionic liquid 1-butyl-2-(4-sulfobutyl)imidazolium-p-toluenesulfonate, which led to 2-MTHF yields of 87%. They further combined the aIL with NH_4PF_6 which increased the yield of 2-MTHF to 92%. The reaction temperature was further increased to 473 K, which led to the conversion of levulinic acid to 2-MTHF with similar selectivity in less than 5 h.

The production of 2-MTHF from γ-valerolactone (GVL) has also been explored. Al-Shaal et al. [105] investigated the hydrogenation of GVL to 2-MTHF over Ru/C. The results indicated that GVL was fully converted, and a maximum 2-MTHF yield of 43% was achieved using no solvent. Another hydrogenation method of levulinic acid into 2-MTHF that involves two-step water removal was shown to have a 90% conversion and a 61% yield of 2-MTHF. Another method for the synthesis of 2-MTHF is patented

by Elliott and Frye [106]. The hydrogenation of angelica lactone with PdRe/carbon catalysts at a temperature range of 473–523 K and 100 atm H_2 produced γ-valerolactone as a first step followed by 1,4-pentanediol, which was further dehydrated to produce 2-MTHF in yields up to 90% [106,107].

A number of studies have focused on the production of 2-MTHF from furfural [42,107,108]. A patented effort was introduced by Ahmed [108], who designed a two-step process for the synthesis of 2-MTHF from furfural via 2-MF. First, furfural is hydrogenated to 2-MF using a Cu-based catalyst at a temperature of 448 K. Then, an Ni-based catalyst is used to transform 2-MF to 2-MTHF at 373 K [107,108]. The hydrogenation of furfural to 2-MTHF was also investigated in the aforementioned study by Zheng et al. [42], using 2-MF as an intermediate. The process resulted in low 2-MTHF yields. The authors attributed this behavior to the difficulty of 2-MTHF separation from the resulting product, because of boiling point similarity with other by-products such as THF, 2-pentanone and water.

An interesting one-step approach for the synthesis of 2-MTHF from pentose sugars was presented by Yang and Sen [109,110]. The process used a soluble rhodium catalyst, hydrogen and Hl/HCl+Nal for the deoxygenation of xylose towards the formation of 2-MTHF. The process achieved a 2-MTHF yield of 80%, which is the highest reported 2-MTHF yield produced from xylose in one step.

Thus, the production of 2-MTHF from platform chemicals such as levulinic acid, GVL and furfural has been explored, with some studies showing promising yields.

Now, the different production methods for a series of furans have been discussed in detail. The next step is to review the most significant studies focusing on the chemical kinetics of oxidation and pyrolysis. These studies use numerical and experimental methods.

3. Theoretical and Experimental Studies of Decomposition and Oxidation

In this section, efforts aimed at understanding the reaction kinetics of furans are discussed with attention to pyrolysis and oxidation. These studies provide insights into the possible reaction rates and pathways and radical formation. The studies can be classified under three categories: (1) quantum chemical kinetic calculations, where theoretical and computational methods are used to capture the reaction kinetics; (2) experimental chemical kinetic studies, where fuels are tested experimentally in flow reactors to determine the rates of reaction and decomposition; and (3) detailed chemical kinetic models, designed to simulate ignition and flame propagation behavior, predicting the reaction pathways.

3.1. Quantum Chemical Kinetic Calculations

Studies involving quantum chemical calculations are discussed here. The main focus of such studies is the theoretical investigation of the decomposition pathways and kinetics of furans, including furan, 2,5-DMF, 2-MF, as well as tetrahydrofurans.

Furan was the main focus for most ab initio studies using various levels of theory [111–113]. One of the earliest efforts was the study by Liu et al. [111], which indicated that the isoxazole unimolecular decomposition channel, which is considered the main decomposition channel of furan, only leads to the formation of the minor products, HC≡CH and H_2O=C=O. The study proposed a new mechanism that can lead to the formation of the more important products CH_3C≡CH and CO. In another study by Liu et al. [112], the experimentally-proposed biradical mechanisms of furan pyrolysis [114] were tested. Good agreement was observed between the calculated activation entropies of the biradical channels and those of non-biradical channels. Furthermore, a furan study by Sendt et al. [113] revealed that the most important pathways occur in parallel. The starting point for the processes was found to be 1,2-H transfers, which lead to the formation of cyclic carbene intermediates as a major channel and lead to the formation of the decomposition products CO and propyne with C_2H_2 and ketene as a minor channel. The study was not able to prove the existence of a significant third channel that leads to the formation of HCO + C_3H_3.

Another furanic fuel, 2-MF, has been studied using quantum chemical calculations [115–117]. Davis and Sarathy [115] employed composite computational methods to determine the bond

dissociation energies (BDEs) for the C–H bond in 2-MF, the enthalpies of reaction and barrier heights of a number of possible initiation reactions. One important finding of this study was that some 1,4 H-migrations have abnormally low barrier height. Furthermore, a new reaction type, referred to as Waddington concerted elimination, was reported. Furthermore, Somers et al. [116] calculated the potential energy surfaces for 2-MF pyrolysis, high-pressure rate constants, $k(T)$, and pressure-dependent rate constants, $k(T, p)$, of elementary reactions. The main pathway for unimolecular decomposition of 2-MF was found to be via H-atom transfers through singlet carbene species, which further undergo ring opening to produce C_5H_6O isomers. Then, the isomers are further decomposed to C_1–C_4 species. The study reported abstraction rate constants show that abstraction from alkyl side chain has the fastest rates. Recently, Hudzik and Bozzelli [117] calculated enthalpies of formation for 2-MF and its radicals, as well as corresponding O–H and O–O BDEs. The results revealed that the BDEs are significantly reduced as a result of the stability of the furan ring coupled with the double-bond-forming capability of the oxygen moiety. With regards to isomers of 2-MF, Zhang et al. [118] performed ab initio calculations to explore mechanism for the OH + 3-methylfuran reaction mechanism among various reaction pathways. The authors suggested that the formation of HC(O)CH=C(CH_3)CHOH and CH(OH)CH=C(CH_3)C(O)H is the main influencing factor of OH + 3-methylfuran reaction and that the influence of direct H abstraction pathways is rather negligible.

2,5-DMF decomposition has also received some attention with regards to quantum chemical studies [10,58,119,120]. The calculations of Simmie and Metcalfe [119] identified the initial steps in 2,5-DMF decomposition as the C–H bond scission in the CH_3 side chain and the formation of β- and R-carbenes. The results revealed the formation of unsaturated species (e.g., allenylketenes) as a result of the furan ring opening. Furthermore, the results indicated that 2-MF is formed through H addition to 2,5-DMF, followed by methyl elimination. Sirjean and Fournet [10] also used theoretical methods to explore important pathways, such as biradical ring opening, initial C–H bond cleavage, H-atom and CH_3-group transfers that involve carbene intermediate species. A detailed chemical kinetic model for 2,5-DMF was developed based on their quantum chemical results. Sirjean and Fournet [120] further investigated the thermal decomposition of 5-methyl-2-furanylmethyl, a major primary radical formed during 2,5-DMF combustion and pyrolysis. The results predicted that the ring-opening of 5-methyl-2-furanylmethyl, followed by the formation of cyclohexadienone by ring enlargement is the favored decomposition channel. The study identified other channels that lead to the formation of linear and cyclic unsaturated C5 species and ultimately to the formation of cyclopentadiene and CO.

Moreover, the reactions of 2,5-DMF with radicals were investigated in a number of studies [121–123]. Potential energy surface for the reaction H + 2,5-DMF → products was calculated by Friese et al. [121], as shown in Figure 5. The results indicated that the main mechanism, with yields over 75%, for the previous reaction is an addition-elimination mechanism to produce 2-MF + CH_3. The same reaction was investigated by Sirjean and Fournet [122], showing that the important pathways in the addition process are the substitution reaction 2,5-DMF + H → 2-MF + CH_3 and the production of 1,3-butadiene and acetyl radical (CH_3CO). The study revealed that the calculated branching ratios are slightly pressure-dependent. Furthermore, Ferraz-Santos and Bauerfeldt [123] used the DFT approach to investigate the potential energy surface for the 2,5-DMF + OH reaction. The results revealed that the formation of a pre-reaction complex in the addition pathways is effective only for temperatures below 550 K. Therefore, the authors inferred that OH addition paths are active under low temperatures, while H-abstraction channels become more dominant under typical combustion conditions.

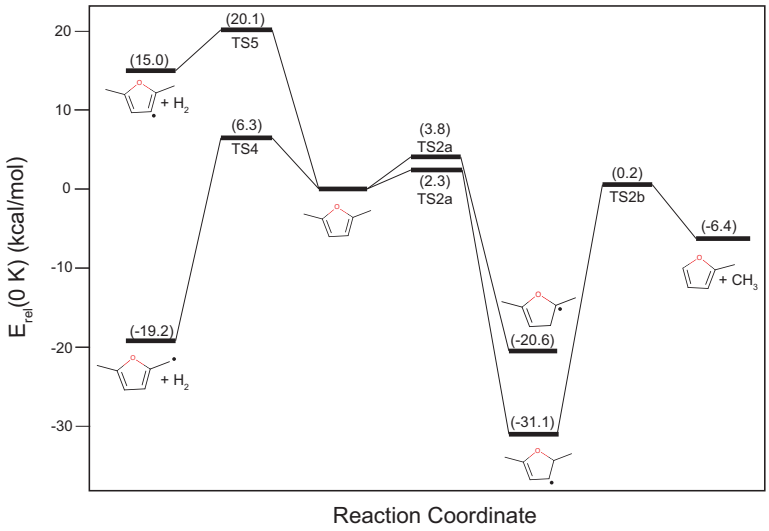

Figure 5. Potential energy diagram for 2,5-DMF + H (adapted from Friese et al. [121]).

In addition to the studies focusing on individual fuels such as furan, 2-MF and 2,5-DMF, another group of studies focused on the chemical kinetics of alkyl furan formation and decomposition [124–128]. One of such efforts is a study by Simmie and Curran [124], in which the room-temperature enthalpies of formation of 2,3-dimethyl-, 2,4-dimethyl-, 3,4-dimethyl-, 2-methyl-, 3-methyl-, 2-ethyl- and 2-vinylfurans were calculated. The results showed good agreement between the calculated and experimentally-measured enthalpies of formation for most of the systems, including furan and 2,5-DMF. However, poor agreement was observed in the case of 2-vinylfuran. These calculations enabled the authors to find the bond dissociation energies (BDEs) of a number of C–H, C–CH_3 and C–OH bonds. The BDE calculations revealed that for alkylfurans, the ring-carbon-H are among the strongest C–H bonds ever recorded, with values of over 120 kcal/mol. Later, Feller and Simmie [125] computed the enthalpies of formation of 2,5-DMF, 2-MF and furan. The results show that the calculated values for the room-temperature enthalpies of formations exhibit good agreement with experimental results. Moreover, Zhang et al. [126] performed quantum chemical kinetic calculations to understand the reaction OH + 2-ethylfuran (2-EF). The results revealed that the dominant mechanism for the OH + 2-EF reaction is the addition-elimination mechanism, while the major products are identified as $CH_3CH_2C(OH)CHCHCHOH$ and $CH_3CH_2COCHCHCHOH$. Furthermore, Smith and Meloni [127] calculated adiabatic ionization energies, photoionization cross-sections and appearance energies of 2-acetylfuran, 2-EF and furfural. The study reported a electronic transition calculated value to the first excited state of the 2-EF cation of 226 kcal/mol, which is in reasonable agreement with the experimental results. Recently, the H abstraction from allylic C–H bonds by $^3O_2$ was investigated for 2-MF and 2-EF by Zhou et al. [128]. The authors claimed that this study is the first attempt to investigate this key type of initiation reactions for compounds containing allylic hydrogen atoms.

Tetrahydrofurans were the focus of another group of computational chemical kinetic studies [26,28,129–132]. For instance, the study by Simmie [26] presented calculations of the entropies, enthalpies of formation, enthalpy functions, specific heats (c_p) and all C–H and C–CH_3 BDEs for THF, 2-MTHF and 2,5-dimethyltetrahydrofuran (DMTHF). The results revealed that at concurrent with the H-abstraction by OH, the formation of some pre- and postreaction weakly bound complexes is observed. Such radicals evolve to well-known intermediates through ring-opening reactions, while dihydrofurans are formed by H-elimination reactions. In another article by Chakravarty and Fernandez [129], the rate coefficients for the hydroperoxyl radical's (HO_2) reaction with 2-MTHF and DMTHF were obtained over a temperature range of 500–2000 K. The high pressure rate constants were found as a function of temperature. The results identified eight transition states for 2-MTHF

and four for DMTHF. The calculated rate coefficients showed that the most favorable path for both 2-MTHF and DMTHF is H abstraction by HO_2 from the C2 position because of its lowest barrier height. Parab et al. [130] sought insight of 3-MTHF combustion kinetics by exploring intramolecular H_2 shift reactions for the alkylperoxy radical (ROO) to hydroperoxyalkyl radicals (QOOH) reactions for eight ROO isomers of 3-MTHF. The study compared the rate constants of ROO isomers of 3-MTHF with their counterparts of methylcyclopentane, which revealed that faster kinetics in 3-MTHF can be attributed to the effect of ring O_2 on the intramolecular hydrogen shift reactions. A similar approach was employed by Parab et al. [131], where the most important abstraction sites were found to be carbon sites neighboring a ring oxygen atom, which was linked to weak C–H bond. Furthermore, Sudholt et al. [28] calculated the BDEs of a number of THFs and explored the initial reactions during the auto-ignition for these fuels. The study revealed that the effect of side chains on the ignitability of furans is minor, while the side chain length strongly affects the ignition behavior. As a result, THFs with a short side chain are more resistant to auto-ignition, and therefore, they are candidates for gasoline replacement, whereas THFs with longer side chains (such as 2-butyltetrahydrofuran) are potential diesel fuels, since they readily auto-ignite. In addition, Antonov et al. [132] reported an experimental and numerical study on the oxidation of THF at 400–700 K. The quantum chemistry calculations revealed that the low temperature pathways of THF are similar to those of alkanes, especially the low temperature chain branching pathways. The most favorable side chain reaction during THF oxidation was HO_2 elimination of peroxy radicals and the decomposition of hydroperoxy radicals, similar to alkanes.

These computational studies have thus provided kinetic insight and thermo chemical data that can help in chemical kinetic model development and/or interpretation; or they explore and compare reaction channels.

3.2. Experimental Chemical Kinetic Studies

In addition to the theoretical and computational efforts aimed at the estimation of rate parameters and main consumption pathways, many efforts have focused on the experimental investigation of combustion events of furans [133]. A large number of experimental studies involved investigations of thermal decomposition in shock tubes and flow reactors [114,134–146]. Other studies were aimed at the exploration of rate constants of furan reactions with important radicals during oxidation [20,132,144,147–152]. Furthermore, a few studies focused on the experimental investigations of furan ionization, speciation and combustion emissions [153–155].

With regards to the decomposition of furans, one of the earliest efforts in this direction was the study by Grela et al. [134], who performed a kinetic investigation of the thermal decompositions of furan, 2-MF and 2,5-DMF under very low pressure conditions of about 1 mTorr in a heatable molecular flow reactor. The results indicated that furan, 2-MF and 2,5-DMF undergo unimolecular decomposition at a temperature range of 1050–1270 K through ring opening reactions. Loss of CO is the only process for furan and 2-MF decomposition, while it is a major one in 2,5-DMF decomposition, among other processes.

The decomposition of furan was later investigated in several studies. In a study by Lifshitz et al. [114] at temperatures of 1050–1460 K in a shock tube, the main decomposition pathway led to the formation of methylacetylene and CO. Another important initiation reaction produces acetylene and ketene. Bruinsma et al. [135] investigated the thermal stability of furan in a flow reactor. The study established that the thermally unstable pathway is the breaking of the C–O bond in the ring. The study also revealed that the temperature dependence of dibenzo compounds of furan is low, and as a result, they are more thermally stable than the parent heterocycles in general. Furthermore, Organ and Mackie [136] used a shock tube along with time-resolved infrared CO_2 laser absorption spectrometry to investigate the pyrolysis of furan diluted in argon over a temperature range 1100–1700 K, at a pressure of 20 atm. The study showed that the rate of furan consumption is first order in furan concentration. The results further indicated that the main decomposition products were C_3H_4

in both propyne and allene forms, acetylene and CO, along with ketene, which was identified by FTIR spectroscopy. In another study by Fulle et al. [137], the unimolecular dissociation of furan was studied in shock tubes equipped with Schlieren densitometry and time-of-flight (TOF) mass spectrometry at a temperature range of 500–3000 K. From the TOF experiments, the branching ratio between 1300 and 1700 K indicated that the major channels are two molecular dissociation pathways to form C_2H_2 + CH_2CO or C_3H_4 + CO. However, the molecular pathway leading to C_3H_4 and CO is favorable at lower temperatures. Furan pyrolysis was also investigated by Urness [138] using a continuous flow silicon carbide tubular reactor. The results showed that the decomposition proceeding through the β-carbene channel opens to the formyl allene intermediate, $CH_2=C=CH-CHO$, and mostly rearranges to $CH_3CCH + CO$ with a little decomposition to $H + CO + HCCCH_2$. Furthermore, at temperatures near 1600 K, up to 10% of the products of formyl allene decomposition are $H + CO + HCCCH_2$, 90% of products are CO and methylacetylene. Recently, Cheng et al. [139] used a flow reactor to investigate the decomposition reactions of furan, such as formation of propyne + CO, acetylene + ketene and propargyl radical over a temperature range of 1100–1600 K at a pressure of 30 Torr. Mole fractions of the pyrolysis products were measured using Synchrotron vacuum ultraviolet photoionization mass spectrometry, as shown in Figure 6. The results indicated that the decomposition of propyne is responsible for the formation of propargyl radical rather than the decomposition of furan, in which propargyl and phenyl radicals are formed.

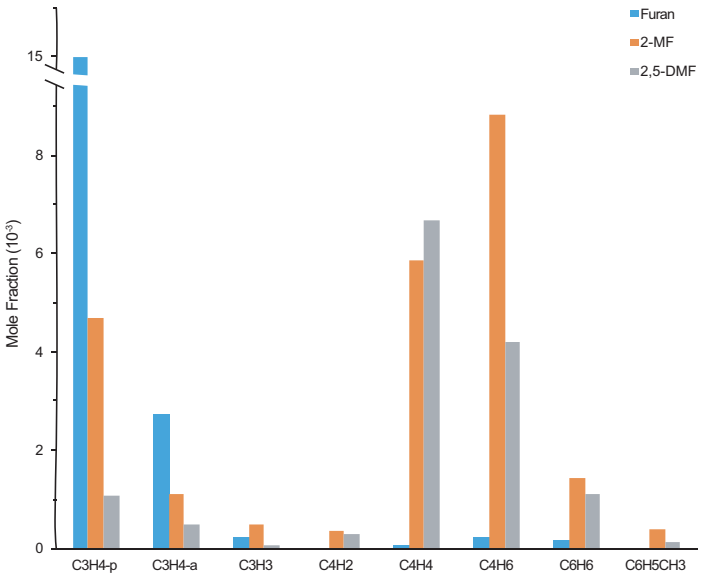

Figure 6. Comparison of measured mole fractions of pyrolysis products 2-MF, 2,5-DMF and furan at 75% fuel conversion (adapted from Cheng et al. [139]).

The decomposition of 2-MF was explored in a few studies. Lifshitz et al. [140] studied 2-MF decomposition in a shock tube over a temperature range of 1100–1400 K. The results revealed two main channels for the decomposition, the migration of 1,2-H atom from C5 to C4 and the transfer of a methyl group from C2 to C3 in the ring. Later, Cheng et al. [141] studied the pyrolysis of 2-MF at temperatures of 900–1530 K and pressures of 30 and 760 Torr. Propargyl radical, methyl radical, 1-butyne and carbon monoxide were identified as main products for the two unimolecular decomposition channels of 2-MF. The study revealed that the pyrolytic decomposition of 2-MF starts by unimolecular decomposition that leads to the formation of propargyl and acetyl radicals. The formation of aromatics was observed to be more significant in 2-MF pyrolysis than in 2,5-DMF pyrolysis. The authors attributed this behavior to the formation of more precursors of aromatics, such as propargyl radical.

With respect to 2,5-DMF, its decomposition was explored in a number of experimental studies, such as the high-temperature study by Lifshitz et al. [142]. The study showed that four C_5H_8

isomers are produced as a result of the transfer of a methyl group from C2 to C3 coupled with the elimination of CO. The study also highlighted the decomposition of 2,5-DMF to C_4H_5 and CH_3CO as an important initiation reaction. The focus on 2,5-DMF continues with a recent study by Djokic et al. [143], which investigates The thermal decomposition of 2,5-DMF over a temperature range of 873–1098 K at a pressure of 1.7 bar in a bench-scale pyrolysis set-up. At low conversions, the main products are H_2, CO, 1,3-cyclopentadiene, CH_4, phenol, 2-MF and a $C_7H_{10}O$ isomer. However, formation of benzene, toluene, indene and naphthalene is observed at high conversion. The results also showed that mono-, di-, tri- and tetra-aromatic products are formed at very high temperatures, which can lead to soot formation. Furthermore, a study on the pyrolysis of 2,5-DMF was performed by Alexandrino et al. [144] at different flow reactor conditions. The results showed that at very high 2,5-DMF concentrations, soot was formed in significant amounts, which needs to be put into consideration when using 2,5-DMF as a fuel additive. Later, Alexandrino et al. [145] investigated the sooting behavior during 2,5-DMF pyrolysis in a flow reactor at a temperature range of 975–1475 K and inlet 2,5-DMF concentrations of 5000–15,000 ppm. The results showed the great impact of temperature on the yields of gas and soot such that more soot is formed at lower temperatures. Moreover, The initial 2,5-DMF concentration was observed to affect the soot yield, but not the gas yield. The authors indicated that maximum soot yields were achieved at high temperatures, especially with higher initial 2,5-DMF concentration, with yields reaching over 60%.

The above studies focused on furan, but tetrahydrofurans have also been experimentally investigated in a number of studies. The pyrolysis of 2-MTHF was recently investigated by De Bruycker [146] in a plug flow reactor at a pressure of 170 kPa, temperatures of 900–1100 K and an N_2/2-MTHF molar ratio of 10. The results indicated that the main pathway for decomposition is by cleavage of the CH_3 group and ring opening to 4-penten-1-ol. The authors indicated that this pathway is different from the main decomposition channel of THF, which is scission of ring bonds. H-abstraction reactions were explored to be the main consumption path for 2-MTHF.

Apart from experimental studies of thermal decomposition, some experimental studies have focused on the study of key reactions. One of these efforts is a study by Elwardani et al. [147], who explored and compared rate coefficients for the reaction of hydroxyl (OH) with furan, 2-MF and 2,5-DMF in a shock tube at temperatures of 890–1388 K and pressures of 1–2 atm. UV Laser absorption techniques were used to monitor the OH radicals. The results revealed that the rate coefficient for 2,5-DMF reaction with OH was the highest, followed by that of 2-MF and furan, which gives insight into the relative reactivity for such fuels. A recent study by Kim et al. [148] presented a new two-step hierarchical mechanism to infer the rate parameters of a target reaction from time-resolved concentration measurements in shock tubes, which was employed to calibrate the parameters of the reaction of OH with 2-MF investigated by Elwardani et al. [147]. Furthermore, 2-MF oxidation in the presence and absence of nitric oxide was investigated by Alexandrino et al. [149]. The study shows that onset temperature of 2-MF consumption is reduced under lean and very lean conditions, both in the absence and in the presence of NO, with more significant temperature reduction occurring in presence of NO. Moreover, it was observed that NO is reduced by reburn reactions at highly rich and stoichiometric conditions, while it is reduced by NO–NO_2 interconversion under lean conditions. Another study on the oxidation of 2,5-DMF was performed by Alexandrino et al. [144]. The results showed high dependence of conversion onset temperature on the equivalence ratio of 2,5-DMF at lean conditions, while 2,5-DMF concentration appeared to have no effect. Increasing the pressure was observed to shift 2,5-DMF conversion onset to lower temperatures. The study revealed the main reaction channels for the conversion of 2,5-DMF, which are H-abstraction from CH_3 group and OH addition to the C2 position, leading to the formation of C_2H_2, CH_3–HCO and CH_3CO radicals. The same group explored the interaction between 2,5-DMF and nitric oxide during oxidation [20] in an isothermal flow reactor at 1 atm over a temperature range of 800–1400 K. 2,5-DMF was observed to have no influence on the NO emissions. Moreover, 2,5-DMF concentrations did not have a pronounced effect on the 2,5-DMF conversion at stoichiometric and rich conditions in the absence or presence of NO.

However, 2,5-DMF concentration effect appeared to be more significant at lean conditions, especially in the absence of NO. Eble et al. [150] also explored the rate coefficients for the reactions of 2,5-DMF + OH and 2-MF + OH in a slow-flow reactor in a pressure range of 7–21 bar. The results indicated no pressure dependence and non-Arrhenius temperature dependence for both reactions. At temperatures between 295–350 K, increasing the temperature led to slightly reduced rate coefficients, while at higher temperatures, rate coefficients decreased more significantly. The authors attributed this behavior to the non-reversible OH addition to the ring in the first regime and the thermal back-dissociation of the OH adduct in the second regime. Most recently, Yoshizawa et al. [151] presented a kinetic investigation of atomic oxygen O(^{3}P) reactions with furan, 2-MF and 2,5-DMF at high temperatures in a shock tube equipped with atomic resonance absorption spectroscopy (ARAS). The study revealed that the rate coefficients are greatest for the atomic oxygen reaction with 2,5-DMF, then 2-MF and, finally, furan.

With regards to the oxidation of tetrahydrofurans, Vanhove et al. [152] investigated the low-temperature oxidation of THF in a jet-stirred reactor (JSR), under atmospheric pressure over a temperature range of 500–1000 K and an equivalence ratio range of 0.5–2.0. The study identified the main products as CO, CO_2, C_1–C_2 compounds, aldehydes, 1-butene, methyl vinyl ether, ethylene oxide, acrolein, furan, propanal, dihydrofuran, 2-butenal, cyclopropanecarboxaldehyde, unsaturated dihydrofuranols and 1,4-dioxene. A significant reactivity of THF was identified at low temperatures, which begins at approximately 550 K, and a negative temperature coefficient zone was observed. Another study by Antonov et al. [132] explored the initiation reactions in low-temperature oxidation of THF. The authors investigated various intermediates and products using time-resolved synchrotron-based vacuum ultraviolet (VUV) photoionization mass spectrometry pressures of 10–2000 Torr and temperatures of 400–700 K. The study indicated that the key reaction sequence is the formation of hydroperoxy-THF-yl radicals (QOOH) from THF-yl peroxy, which is followed by a second O_2 addition then two decomposition pathways to either γ-butyrolactone hydroperoxide + OH or dihydrofuranyl hydroperoxide + HO_2. The degree of branching is determined from the competition between these two decomposition pathways.

A few studies focused on the ionization of furans. Jiao et al. [153] employed Fourier transfer mass spectrometry (FTMS) to reveal ion chemistries in 2,5-DMF related to plasma-assisted ignition and combustion. The results showed that electron ionization of 2,5-DMF results in the formation of five ions in an energy range of 10–200 eV: $C_6H_8O^+$, $C_6H_7O^+$, $C_5H_5O^+$, $C_4H_5^+$ and $C_2H_3O^+$, with their neutral forms being H, CH_3, H + CO and H + C_4H_4, respectively. The results also showed that the total ionization cross section has a maximum value of 1.7×10^{-15} cm^2 at ~90 eV. It was found also that the ions $C_2H_3^+$, $C_2H_3O^+$ and $C_5H_3O^+$ react with 2,5-DMF via mechanisms that include H^- transfer, charge transfer and H^+ transfer.

With regards to experimental exploration of pollutant emissions, Wu et al. [154] investigated the formation of polycyclic aromatic hydrocarbons (PAH) during furan and 2-MF pyrolysis using pyrolysis-gas chromatography-mass spectrometry at a temperature of 1373 K. The results revealed the effect of various side chain functional groups on the products formed. The hydroxyl group as a side chain functional group leads to the formation of dimers, while an aldehyde group leads to the formation of pyrans. However, the results show that the mechanism of furan decomposition and ring opening is unified for all furans investigated.

Moreover, the speciation of furans was studied by Tran et al. [155], who reported a full systematic speciation dataset for 2,5-DMF, 2-MF and furan over a temperature range 730–1170 K and different equivalence ratios in a flow reactor at 1 bar. The reactants, intermediates, and products were further analyzed by means of electron ionization molecular-beam mass spectrometry. An extended chemical kinetic model was developed from experimental data to include the low-to-moderate-temperature oxidation chemistry.

The experimental studies reviewed above provide valuable results on the decomposition, oxidation, radical and pollutant emission, as well as ionization of furans. Such information can support

the development and improvement of chemical kinetic models, for better predictive performance. The progress of the modeling efforts of furans will be discussed next.

3.3. Detailed Chemical Kinetic Models

In this part, efforts aimed at the detailed chemical kinetic modeling of different furans are demonstrated. These efforts benefit from the rate parameter and pathway data obtained from the experiments and calculations reviewed above. The proposed chemical kinetic models can be classified into models of furan, alkyl furans and tetrahydrofurans. Moreover, a few models were developed as combined models for the simulation of the combustion properties of multiple furans, as well as blends of furans with other conventional fossil fuels. These models were not only developed to predict key combustion properties such as laminar burning velocities and ignition delay times, but also to enable further chemical kinetic exploration, through sensitivity and reaction pathway analyses.

Furan has been the focus of modeling efforts for a long time [8,113,136]. One of the earliest efforts was the study by Organ and Mackie [136], in which a 46-reaction kinetic model for the pyrolysis of furan was presented and tested against the observed products concentration profiles, showing good agreement. In another study by Sendt et al. [113], an updated chemical kinetic model was developed for furan based on the experimental data reported by Organ and Mackie [136]. Model predictions agreed with species concentration profiles obtained experimentally in shock tubes [113,156]. Furthermore, Tian et al. [8] developed a detailed model of 206 species and 1368 reactions comparing its predictions with observed mole fraction profiles for three laminar furan flames, with reasonable agreement. The resulting model was used to explore the main pathways for furan consumption at various equivalence ratios, through rate-of-production and sensitivity analyses. Moreover, literature shock tube pyrolysis results were used for model validation, also showing reasonable agreement [8,156].

Chemical kinetic models have also been proposed for 2-MF [11,140]. Lifshitz et al. [140] proposed a reaction mechanism of 36 species and about 100 elementary reactions for the modeling of the thermal decomposition of 2-MF over a temperature range of 1100–1400 K. The modeling results indicated that the calculated mole percentage of 2-MF and its decomposition products has a satisfactory agreement with experimental data. The authors rationalized the simulated product distribution by assuming that a methyl group migrates from ring position 2 to position 3. An important effort was performed by Somers et al. [11] who presented a chemical kinetic model for 2-MF oxidation based on ignition delay time and laminar burning velocity data. The detailed chemical kinetic model consists of 2059 reactions and 391 species, with good agreement observed with experimental data. However, the model under-predicted ignition delay times for lean conditions at temperatures below 1400 K. The sensitivity and rate of production analyses results highlighted the importance of reactions of hydrogen atom with 2-MF, including abstraction which enhances 2-MF reactivity and addition to the furan ring which negatively affects the reactivity.

One of the most promising furans as fuels is 2,5-DMF. As a result, a number of its kinetic models have been proposed [9,10,142,144]. The first 2,5-DMF kinetic model of 50 species and 181 elementary reactions was presented by Lifshitz et al. [142]. The next major work was the detailed kinetic model of 2,5-DMF oxidation by Sirjean et al. [10], incorporating results of quantum chemical calculations. Model validation was performed against ignition delay time measurements in a shock tube at pressures of 1 and 4 bar and temperatures of 1300–1831 K, as well as the 2,5-DMF pyrolysis species concentrations reported by Lifshitz et al. [142]. The results showed good agreement between model predictions and experimental data, especially with respect to ignition delay times. An extensive chemical kinetic model was then developed by Somers et al. [9]. The model contains 2768 reactions and 545 species, and it was developed to simulate 2,5-DMF ignition delay time and pyrolysis experiments performed in a single-pulse shock tube; laminar burning velocity data; and speciation measurements performed in a jet stirred reactor. The simulation results showed that model reproduced the experimental data accurately. The model was used to further explore the main consumption pathways of 2,5-DMF. It was found that a 3–2 H atom transfer reaction is the most favorable unimolecular decomposition channel of

2,5-DMF at high temperatures. Among the important reactions identified by the study are the H atom reactions with the fuel, which are crucial in predicting pyrolysis and ignition delay times. Furthermore, another detailed chemical kinetic mechanism was constructed by Alexandrino et al. [144] based on the 2,5-DMF submechanism developed by Sirjean et al. [10] and updated with new oxidation and pyrolysis data. Generally, experimental results were consistent with model predictions.

Chemical kinetic models of tetrahydrofurans have been proposed [27,146,157,158]. The first 2-MTHF model by Moshammer et al. [27] was developed based on mole fraction profiles of products, reactants and a number of intermediate species including radicals obtained experimentally for premixed low-pressure 2-MTHF flames at an equivalence ratio of 1.7. The proposed model consists of 185 species and 1412 reactions, including 2-MTHF sub-mechanism. Good qualitative agreement was generally observed with the experiments for the major species and for intermediate species. However, the quantitative agreement is poor for most species. Then, De Bruycker et al. [146] presented another 2-MTHF kinetic model, developed with the help of new advanced theoretical calculations. The authors segment the new model into three main mechanisms: a primary mechanism, covering the oxidation and pyrolysis of 2-MTHF and its radicals; a base mechanism, capturing the oxidations and pyrolysis of small oxygenates and hydrocarbons; and a secondary mechanism, focusing on 2-MTHF decomposition products. The authors compare the new model with that of Moshammer et al. [27], claiming that the primary 2-MTHF reactions and decomposition reactions of 2-MTHF radicals are described in more detail in the new model, based on the fact that those were obtained from calculations at the complete basic set CBS-QB3 level of theory. The model exhibited good agreement with experimental data for mole fraction profiles and laminar burning velocities, with the model slightly over-predicting laminar burning velocities. Another detailed chemical kinetic model for 2-MTHF was proposed by Fenard et al. [157], based on measurements of ignition delay times and mole fraction profiles in a rapid compression machine. The proposed model consists of 507 species in 2425 reactions. The model was validated for the oxidation of 2-MTHF against experimental data, where the validation was extended to higher temperatures using existing ignition delays and low pressure laminar flame speciation data. Reaction pathway and sensitivity analyses revealed that the prediction of ignition delay times depends on the balance between the different radicals resulting from H abstraction. Further, Tran et al. [158] developed a detailed kinetic model for THF combustion. The authors used an automatic model generation tool (EXGAS), Evans–Polanyi correlations and CBS-QB3 theoretical calculations. The model simulations exhibit good qualitative agreement with experimental results of ignition delay times and laminar burning velocities. However, the model quantitatively over-predicts ignition delay times, especially at higher temperatures. It also generally over-predicts laminar burning velocities.

In addition to models of individual furans, other models were developed to include mechanisms of multiple furans [149,159–161], as well as fossil fuel surrogates [25]. An important effort was a single kinetic model with 305 species in 1472 reactions that was used to simulate the flame structure of furan [159], 2-MF [160] and 2,5-DMF [161] based on the work on Sirjean et al. [10]. The model predictions are compared to experimentally-measured laminar burning velocities of the three fuels, showing qualitative agreement only. With regards to furan, it was observed that the key furan consumption channel is started by H-addition on the carbon atom next to the O-atom producing acetylene [159]. For 2-MF, the main consumption pathways were found to be ipso-addition and H-abstractions from the methyl group [160]. The main finding with regards to 2,5-DMF was its increased ability to form 1,3-cyclopentadiene and benzene, precursors to soot, relative to the less substituted furans [161]. Later on, three different 2-MF reaction sub-mechanisms were incorporated into the 2,5-DMF chemical kinetic model by Alexandrino et al. [144] to create an updated version that captures the reaction kinetics of 2-MF, as well as 2,5-DMF [149].

In a study by Eldeeb and Akih-Kumgeh [25], a combined model for 2,5-DMF and *iso*-octane combustion was developed, based on existing chemical kinetic models for the pure components [9,162]. This was the first effort with regards to the kinetic modeling of furan-gasoline blends. The authors performed reaction rate modifications to improve the predictive accuracy of the combined model with

new and previous ignition data. The resulting model contained 3691 reactions among 686 species. The results showed that the model predicted the relative ignition trends of the pure fuels and blends.

This concludes the discussion of the efforts aimed at understanding the reaction kinetics of furan-based fuels. As can be observed, kinetic models of individual furans as well as multiple furans are emerging. In the next section, the focus is shifted to experimental characterization of furanic combustion properties in engines and canonical experiments for ignition and flame studies.

4. Characterization of Furan Combustion Properties

This section starts with a review of different studies of furan-based fuels in engines. Then, the auto-ignition characterizations will be discussed, including individual and comparative ignition delay time studies, in shock tubes and rapid compression machines. Finally, characterization of laminar burning velocities of furan-based flames will be reviewed. The studies discussed in this section reflect the increased interest in furans as possible fuels or fuel additives.

4.1. Engine Studies

The increased interest in the mass-production of oxygenated biofuels has prompted the testing of these fuels in practical engines. Generally, the properties of 2-MTHF, 2,5-DMF and 2-MF suggest that they are suitable for use in low-concentration blends with gasoline (i.e., $\leq$10%) for standard vehicles, while their concentrations can be increased when used in flex fuel vehicles [34]. However, special care in the evaluation of emissions and environmental impact is needed, since 2,5-DMF and 2-MF in particular have high toxicity levels [34]. Some of the engine studies focused on individual furans and compared their performance with other conventional fuels and biofuels. Other studies tested the performance of blends of furans with conventional fuels, such as gasoline and diesel. Moreover, a number of studies performed comparative engine investigations of individual furans.

A number of engine studies of individual pure furans investigated the performance of 2-MF [18,163–166]. Thewes et al. [163] investigated the impact of using 2-MF on engine performance and in-cylinder spray evaporation and formation in a direct-injection spark-ignition (DISI) single-cylinder research engine. The 2-MF results were compared to those of gasoline with a research octane number (RON) of 95 and ethanol. The results showed that 2-MF exhibits quicker evaporation than ethanol. 2-MF also showed excellent combustion stability at cold conditions, with about 61% reduction in HC emissions compared to conventional gasoline. Furthermore, 2-MF exhibited better knock resistance than gasoline at full load, which allows for increasing the compression ratio in newer engines and therefore the efficiency by up to 9.9%. However, the knock resistance of 2-MF was shown to be lower than ethanol. Furthermore, the results highlighted one disadvantage of using 2-MF, which is an increased level of NO_x emissions. Furthermore, Pan et al. [18] further evaluated the performance of 2-MF in a single-cylinder SI research engine under stoichiometric conditions. The study focused on the effect of compression ratios (CR) of 8, 9 and 10 and exhaust gas recirculation (EGR) rates of 0–15% on the combustion behavior and emissions of 2-MF compared to gasoline. 2-MF exhibited higher NO_x emissions, cylinder pressure, combustion temperature and knocking intensity than gasoline. The study indicated that using EGR resulted in improvement of the combustion and emissions, mainly as a result of knock suppression and lower NO_x emissions. At an EGR rate of 15%, 2-MF exhibited a 31.2% higher indicated thermal efficiency than gasoline at a CR of 10. 2-MF was also tested in a single-cylinder DISI research engine and compared with 2-butanone, ethanol and conventional RON95 gasoline by Hoppe et al. [164]. The auto-ignition resistance of 2-MF was observed to be similar to ethanol but lower than 2-butanone. Furthermore, 2-MF exhibited a higher vapor pressure, a lower heat of vaporization and a better primary droplet breakup than ethanol. The results indicated that the combustion stability of 2-MF can result in higher knock resistance than gasoline [164–166]. At a higher compression ratio, an efficiency increase of up to 19% could be achieved with 2-MF compared to gasoline [164–166]. However, 2-MF and 2-butanone exhibited higher levels of NO_x emissions than ethanol, but the PM emissions were significantly reduced compared with gasoline.

Engine testing of 2-MF was extended to include its blends with gasoline [15,167–170]. Gouli et al. [15] investigated the ignition quality of 2-MF blends with gasoline in a cooperative fuel research (CFR) engine. The results indicated that furan derivatives such as 2-MF, furfuryl alcohol and furfurylamine have a very desirable antiknock effect when added to gasoline compounds. In addition, it was found that the addition of 2-MF and furfurylamine resulted in a reduction in HC and CO emissions compared to pure gasoline at the same air-to-fuel ratio. In another study by Wei et al. [167], the combustion and emissions characteristics of a 10% 2-MF by volume blend with gasoline (M10) were compared with pure gasoline and an ethanol/gasoline blend (E10), in a four-stroke single-cylinder spark ignition engine at stoichiometric conditions. A relatively high in-cylinder maximum temperature and pressure was observed when M10 was used, which is due to its shorter combustion duration. Moreover, M10 exhibited a slightly higher torque and brake power and lower brake specific fuel consumption than E10. M10 was also observed to produce lower HC and CO emissions than gasoline, with higher NO_x observed due to M10's higher combustion temperature. Moreover, Wei et al. [168] investigated the spray characteristics of 20% and 40% by volume fraction 2-MF/gasoline blends (M20 and M40) and pure gasoline in a six-hole direct-injection (DI). Two distinct spray shapes, namely flash boiling and non-flash boiling, were observed. The spray area was observed to increase for the flash boiling shape with higher 2-MF mixing ratios and lower fuel temperatures at low ambient pressures. However, increasing the 2-MF mixing ratio resulted in reduced spray penetration in the non-flash boiling case. Later, Sivasubramanian [169] investigated the combustion and emissions of three different blends of 2-MF with unleaded gasoline (M10, M20 and M30) along with pure gasoline in a four-stroke MPFI SI engine. The results indicated that higher 2-MF concentration in the blend resulted in lower CO and HC emissions and higher brake thermal efficiency and NO_x emissions. Slight retarding of the ignition timing by a 2° crank angle (CA) for NO_x reduction purposes was observed to reduce the brake thermal efficiency, as well. Recently, pure 2-MF, as well as 2-MF blends with gasoline (10% and 20% by volume) were studied by Wei et al. [170] in a single-cylinder SI engine at loads of 7–11 bar indicated mean effective pressure (IMEP), 1500 rpm and stoichiometric conditions. The results were compared to those of RON 97 gasoline, with the focus given to the performance of cyclic variation of 2-MF and its blends with gasoline, as well as the effects of compression ratio, ignition timing and EGR. Generally, the results highlighted the desirable characteristics exhibited by pure 2-MF and low 2-MF concentration blends with gasoline, with respect to decreasing cyclic variation, revealing that the retarded spark timing and high EGR rates further enhanced this behavior.

Moreover, the performance of 2-MF blends with diesel in compression-ignition (CI) engines has been studied. Xiao et al. [171] investigated the combustion and emissions of 2-MF/diesel blends relative to pure diesel in a four cylinder direct-injection compression-ignition engine. The study indicated a retarded combustion phase of the blends as a result to the higher 2-MF content. Furthermore, higher auto-ignition resistance, shorter combustion duration and higher brake thermal efficiency were observed for the 2-MF/diesel blends compared with pure diesel. Higher NO_x and significantly lower soot emissions were observed with 2-MF blends than pure diesel. With respect to CO and HC emissions, similar levels were observed at medium and high loads, while 2-MF/diesel blends have higher CO and lower HC emissions than pure diesel at lower loads.

The engine performance of 2,5-DMF has been extensively investigated [12,172–176]. Zhong et al. [12] tested the performance of 2,5-DMF, compared with that of ethanol and gasoline in a single-cylinder gasoline direct-injection (GDI) research engine at mean effective pressures of 3.5–8.5 bar. The authors reported very promising results for 2,5-DMF as a prospective biofuel, with combustion and emissions performance similar to those of gasoline. 2,5-DMF exhibited an initial combustion duration that was shorter than that of gasoline. Furthermore, engine knock occurred in the case of 2,5-DMF at loads higher than those attainable with gasoline knock-free. Furthermore, in a study by Daniel et al. [172], 2,5-DMF was tested in a DISI engine and compared with gasoline and ethanol using optimized spark timings. The results indicated that 2,5-DMF has a higher burning rate, shorter initial combustion duration, greater combustion efficiency and lower HC and CO emissions compared with gasoline.

The authors concluded that based on the study results, 2,5-DMF is not only a gasoline additive, but also a renewable gasoline alternative. Another effort by Daniel et al. [173] investigated the individual HC and carbonyl species emitted from 2,5-DMF combustion using liquid chromatography and gas chromatography mass spectrometry in a single cylinder DISI engine at stoichiometric conditions. The results indicated that unburned 2,5-DMF is the major species emitted, while cyclopentadiene, methyl vinyl ketone, 2-MF and aromatics are among the main emissions. The results also indicated that emissions of linear alkanes are minimal, except for methane. Most importantly, 2,5-DMF was shown to exhibit the lowest carbonyl and formaldehyde emissions compared with gasoline, ethanol, methanol and *n*-butanol. Moreover, Daniel et al. [174] further examined the combustion performance and emissions levels of 2,5-DMF at the optimum spark timing of 10 crank angle degrees retard in a DISI engine. The spark sensitivity of 2,5-DMF at a full load was below gasoline and butanol, but greater than ethanol and methanol. The results indicated that the spark window was observed to be wider in the case of 2,5-DMF, as well as the other biofuels. This was attributed to better knock resistance and greater charge-cooling. This behavior led to more efficient reduction in CO_2 emissions than in gasoline. More importantly, 2,5-DMF was observed to be the only investigated biofuel to exhibit exhaust gas temperatures as high as those for gasoline. This enables rapid catalyst light-off, while the combustion stability is maintained. The results indicated that 2,5-DMF is promising as an effective cold-start fuel.

Further 2,5-DMF testing was performed by Daniel et al. [175], with focus on sensitivity to engine control parameters, including the timing of ignition and injection, valve timing and relative air-fuel ratio. The results indicated that 2,5-DMF exhibits lower sensitivity to main engine parameters, compared to gasoline. This reduced sensitivity leads to a bigger emission optimization as the optimal indicated mean effective pressure can be retained across a wider range of the engine parameters. Furthermore, PM and soot emissions from 2,5-DMF were studied by Wang et al. [176] in a single-cylinder DISI research engine using thermogravimetric analysis (TGA). The results indicated that PM emission from 2,5-DMF are mainly due to volatile components, with soot accounting for only 35% of PM emissions at 8.5 bar IMEP. However, ethanol exhibits better soot emission percentage of 6.3% of PM emissions. Furthermore, 2,5-DMF was observed to have an intermediate reaction rate of soot oxidation between that of ethanol and gasoline.

The engine performance of 2,5-DMF as an additive to gasoline has been investigated in several studies [13,14,177–180]. Tian et al. [177,178] investigated the spray characteristics of pure 2,5-DMF and its blends with gasoline, such as droplet size distribution, spray penetration and droplet velocity. The results indicated that 2,5-DMF and its blends exhibited spray properties similar to gasoline. Compared to ethanol, 2,5-DMF had smaller droplets than ethanol, which get smaller much faster at higher injection pressures. Furthermore, 2,5-DMF had a higher mean velocity of spray droplets than ethanol, while it was similar to that of gasoline. Overall, the authors concluded that 2,5-DMF possesses more favorable spray characteristics than ethanol while it is comparable to gasoline [177]. Furthermore, the authors indicated that employing more advanced spark timing at high load leads to better engine performance of 2,5-DMF. However, they stated that 2,5-DMF generally exhibits similar fuel consumption, similar HC and CO emissions, but higher NO_x emission than gasoline [178]. Another article by Wu et al. [179] investigated a flexible, dual-fuel concept of dual-injection in a single-cylinder SI research engine. Port fuel injection (PFI) was applied to gasoline, while direct injection (DI) was used for 2,5-DMF. The results showed that the combustion duration was significantly reduced when 2,5-DMF mass fraction is increased in DI. Using 2,5-DMF as the DI fuel also led to reduced HC emissions, but increased NO_x and CO_2 emissions. The dual-injection concept was further investigated by Daniel et al. [13] for a 2,5-DMF/gasoline blend called D25, containing 25% 2,5-DMF in gasoline, by volume. The results showed reduced combustion durations and increased in-cylinder pressures in the case of dual-injection compared to DI. This resulted in a 4% increase in thermal efficiencies and 3.2% decrease in fuel consumption. Another important finding was that the fuel consumption rate with dual-injection for D25 was 1.2% lower than pure gasoline in DI at a load of 8 bar IMEP. Later, the knocking behavior of 2,5-DMF/gasoline blends with 2,5-DMF volume

percentages between 5–15% was investigated by Rothamer and Jennings [14] in a single-cylinder DI research engine. All 2,5-DMF blends exhibited better knock-limited spark advance (KLSA) compared to gasoline. The study indicated that the best performance was obtained using the 10% 2,5-DMF blend, as well as the 10% ethanol blend, with both blends improving the KLSA of seven crank angle degrees under full load conditions. However, 2,5-DMF exhibited lower knock resistance than ethanol at similar volumetric blend percentages because of ethanol's higher latent heat of vaporization that led to a lower in-cylinder temperature. Another study by Shukla et al. [180] investigated the performance and emission characteristics of a 5% 2,5-DMF blend in gasoline (DMF5G) compared to a 10% ethanol blend in gasoline (E10G) in a small-carbureted SI electrical generator set. DMF5G was shown to be better-suited to cold start combustion than E10G as it has similar distillation behavior to gasoline, thereby reducing cold start emissions. DMF5G was also shown to reduce emissions of CO, HC and NO relative to those of gasoline, as shown in Figure 7.

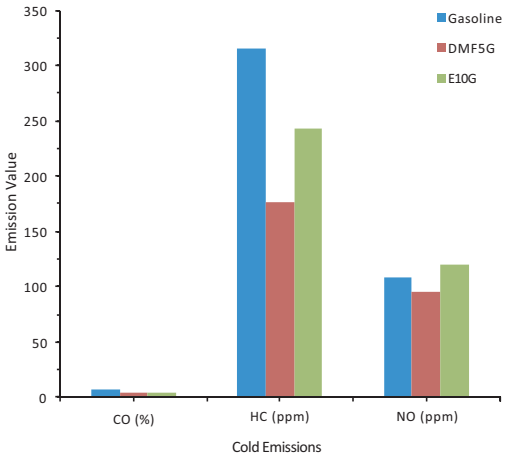

Figure 7. Comparative cold emission of pure gasoline compared to a 5% 2,5-DMF blend in gasoline (DMF5G) and a 10% ethanol blend in gasoline (E10G) (Adapted from Shukla et al. [180]).

The possibility of using 2,5-DMF as a diesel fuel additive has also been investigated [181–190]. Chen et al. [181] studied the performance of 2,5-DMF blends with diesel in a a multi-cylinder CI engine at a volumetric percentage of 30%. The study revealed that the 2,5-DMF blend had the longest ignition delay times, resulting in higher rate of pressure rise and faster burning rate. Using higher rates of EGR, 2,5-DMF exhibited superior soot emission reduction to *n*-butanol and gasoline blends with diesel, mainly as a result of its long ignition delay times and atomic oxygen. The performance of 2,5-DMF in diesel engines was further investigated by Liu et al. [182]. Blends of diesel with 20% volumetric blending ratio of 2,5-DMF (DMF20), cetane and *iso*-cetane, *n*-heptane and 2,5-DMF mixture with 2-ethylhexyl nitrate were tested at EGR rates of 0–62%. Results indicated that DMF20 exhibited more premixed combustion due to low cetane number and the effect of oxygen. However, the fuel oxygen was the main reason for higher NO_x emissions of DMF20, while the addition of 2,5-DMF did not affect HC and CO emissions. The performance of DMF20 was also compared in another study by Liu et al. [183] to that of a 20% blend of *n*-butanol in diesel at the same conditions. DMF20 had higher NO_x emissions especially at lower EGR rates, while it has lower soot emissions and soot luminosity than the butanol blend. Another effort was presented by Zhang et al. [184], in which a 2,5-DMF/diesel blend was tested and compared with gasoline in a modified single cylinder CI engine at low temperatures. The results indicated that soot formation and the soot-NO_x trade-off relationship were almost eliminated at 2,5-DMF content up to 40%. However, CO and HC emissions seemed to be unaffected by 2,5-DMF addition. The authors concluded that differences in fuel oxygen and ignition delay times and are the main reasons for deviation in combustion and emission characteristics of 2,5-DMF and gasoline. In spite of the aforementioned advantages of 2,5-DMF/diesel blends, they tend

to increase combustion noise. A study by Zhang et al. [185] investigated the effect of the addition of 2% 2-ethylhexyl nitrate (EHN) to a 2,5-DMF/diesel blend with 40% 2,5-DMF by volume. The results revealed that the EHN addition resulted in an 80% reduction in peak soot emission, while the maximum pressure rise rate was same as diesel. Most importantly, the addition of EHN to 2,5-DMF/diesel blends helped to decrease combustion noise while maintaining low soot emissions. In another study by Chen et al. [186], it was shown that 2,5-DMF addition to diesel led to longer ignition delay time and smoke reduction, especially at higher EGR rates. The trade-off between soot and NO_x emissions was shown to be minimal or non-existent at a 2,5-DMF fraction of 40%. The combustion and emissions of 2,5-DMF/diesel blends were investigated by Liu et al. [183] compared with diesel blends with other fuels. The results identified fuel cetane number as the main factor impacting the auto-ignition behavior. 2,5-DMF blends with diesel were observed to cause the greatest NO_x emissions among the blends at lower EGR rates. The results also revealed that the addition of 2,5-DMF to diesel results in lower soot luminosity than that of butanol/diesel blends. Xiao et al. [187] also investigated 2,5-DMF/diesel blends. The results showed that increasing the 2,5-DMF fraction in the blend leads to a significant increase in the maximum heat release, along with a noticeable decrease in the peak cylinder pressure at 0.38 MPa brake mean effective pressure (BMEP). Changing the load to 0.63 MPa BMEP reverses the effect of 2,5-DMF content on the peak cylinder pressure. Adding 2,5-DMF to diesel was observed to generally reduce PM concentration. Moreover, the use of 2,5-DMF/diesel blends was observed to slightly increase the NO_x emissions, brake thermal efficiency and brake specific fuel consumption compared with using pure diesel fuel [188]. The combustion and emissions of three oxygenated ring HCs considered as diesel additives, including 2,5-DMF, were studied in a single-cylinder diesel engine by Zheng et al. [189]. The results showed that blends containing 2,5-DMF have the longest ignition delay times. The 2,5-DMF/diesel blend also exhibited the lowest soot emissions, which further leads to increased combustion and thermal efficiencies. Furthermore, Wei et al. [190] investigated the combustion and emission performance of diesel blends with 0–30% 2,5-DMF in a four-cylinder diesel engine. With respect to PM emissions, the number of accumulation mode particles was observed to decline when 2,5-DMF was added to diesel, but the number of nucleation mode particles, more harmful to humans and the environment, increased, which further leads to lower geometric mean diameter of particles.

Other studies have focused on the comparative engine performance of pure furans, as well as their blends with gasoline and diesel [16,191]. Christensen et al. [16] tested the effect of blending oxygenates, including 2-MF, 2,5-DMF and 2-MTHF with gasoline at oxygen levels up to 3.7%. Physical and chemical properties of the blends, including octane rating, were compared to the American Society for Testing and Materials (ASTM) specifications for SI engine fuels to evaluate the possibility to use them as gasoline additives. The study indicated that 2-MF, 2,5-DMF were the only oxygenates examined along with ethanol to exhibit satisfactory octane ratings. However, 2-MTHF was one of two oxygenates that did not cause an increase in octane rating when added to gasoline. Another article by Wang et al. [191] compared the performance of 2-MF to that of 2,5-DMF, gasoline and ethanol in a spray-guided single-cylinder DISI engine at stoichiometric conditions. The study focused on the regulated CO, HC, NO_x and PM emissions, as well as other unregulated emissions, such as formaldehyde and acetaldehyde. The results indicated that 2-MF possesses similar knock resistance to that of 2,5-DMF and better that that of gasoline. Moreover, 2-MF exhibited an indicated thermal efficiency about 3% higher than gasoline and 2,5-DMF at all test conditions. Furthermore, it was shown that 2-MF exhibited nearly 30% lower volumetric specific fuel consumption than ethanol, while the regulated emission levels were similar to other fuels in the study. However, 2-MF was observed to have much lower aldehyde emission than gasoline and bio-ethanol.

Noteworthy is that the engine studies of tetrahydrofurans in general are scarce. One study by Nasrullah and Gopal [192] tested the effect of adding THF to methyl ester of Jatropha oil (MEJO) as a CI engine fuel to evaluate the engine performance. The results indicated that 2% THF added to MEJO maximized the brake thermal efficiency and minimized brake specific fuel consumption relative

to pure MEJO. The same blend was observed to achieve the minimum CO, HC and NO_x emissions. Moreover, the same blend exhibited a smoke density reduction by 14.3% compared with diesel.

The previous discussion focused on the characterization of general combustion and emission characteristics of furan-based fuels in both SI and CI engines. Generally, cyclic compounds are the preferred octane boosters for modern SI engines, as they exhibit favorable knock-resistance [193], confirmed by engine studies using 2-MF and 2,5-DMF. Moreover, engine studies show that alkyl furans exhibit lower CO, HC, PM and soot emissions than conventional fuels. On the other hand, 2-MF and 2,5-DMF were generally observed to have higher NO_x emissions than conventional fuels. However, further engine performance characterizations of THFs, especially 2-MTHF, are needed to evaluate their potential as biofuels. In the following subsection, the focus is on the auto-ignition behavior of such fuels, as an important indicator of the global reactivity of these fuels and, therefore, their suitability for use in different engine types.

4.2. Characterization of Auto-Ignition Behavior of Furans

As furans are considered a promising class of biofuels, their auto-ignition behavior is an important feature to investigate. In the literature, a number of ignition studies of such fuels focused on individual behavior, while others attempted to systematically establish relative reactivity trends, as the choice of engine fuels is mainly dependent on relative properties [194]. These established trends are also crucial in the improvement of existing chemical kinetic models. Therefore, the differences in reactivity elucidated by ignition investigations of these compounds enable further understanding and modeling.

The main method for auto-ignition characterization is performing ignition delay time studies, which can be used to establish fuel reactivity trends and validate proposed models. The main experimental methods to measure ignition delay times are using shock tubes and rapid compression machines (RCM). Despite the greater focus on production methods and engine studies of furans, interest in auto-ignition studies has been increasing recently. In this part, we review the experimental studies of the auto-ignition behavior of furan-based fuels, either as individual studies or as comparative studies that establish relative trends.

4.2.1. Ignition Delay Times of Furans

With regards to auto-ignition investigations of furan [195], an initial study was performed by Wei et al. [23] at pressures of 1.2–10.4 atm and temperatures of 1320–1880 K for mixtures with furan concentrations of 0.25–1% diluted in argon and equivalence ratio range of 0.5–2.0. An ignition correlation was proposed as a function of temperature, pressure and equivalence ratio. However, this correlation is limited to dilution level used and fails to predict at much higher or lower O_2 levels.

The ignition behavior of 2-MF has been more extensively studied [11]. For instance, Somers et al. [11,22] performed shock tube ignition delay time measurements of 2-MF/O_2/Ar mixtures at a pressure of 1 atm and an equivalence ratio range of 0.5–2.0 over a temperature range of 1200–1800 K. A chemical kinetic model was developed based on the experimental data. Another high temperature ignition study of 2-MF was performed by Wei et al. [21] at pressures up to 10.65 bar, temperatures of 1120–1700 K and equivalence ratios of 0.25–2.0. The measurements indicated a negative effect of pressure and a positive effect of dilution ratio on ignition delay times. Moreover, a crossover was observed in the ignition delay time relationship with equivalence ratio. Further, a high pressure shock tube ignition study by Uygun et al. [22] was performed for stoichiometric 2-MF/air mixtures at a pressure of 40 atm and temperatures of 820–1215 K. The results revealed a relatively long and gradual pressure rise before the main ignition event, as well as far-wall ignition events at low temperatures. Furthermore, a rectangular shock tube was used to investigate the ignition behavior of a 2-MF/O_2/Ar mixture at 10 bar and stoichiometric conditions over a temperature range of 871–1098 K. The results show that ignition at temperatures below 940 K begins as flame kernels and ends in the form of explosion.

Besides furan and 2-MF, a number of investigations of the auto-ignition behavior of 2,5-DMF were carried out [9,10]. In a study by Sirjean et al. [10], ignition delay times were measured for 2,5-DMF/O_2/Ar mixtures in a shock tube at temperatures of 1300–1831 K, pressures of 1.0 and 4.0 atm and equivalence ratios of 0.5–1.5. Based on the results, a detailed chemical kinetic model was developed, as mentioned earlier. An improved chemical kinetic model was presented by Somers et al. [9], based on a new set of ignition delay time measurements for 2,5-DMF/O_2/Ar mixtures at an equivalence ratio range of 0.5–2.0, temperatures of 1350–1800 K and pressures of 1, 20 and 80 atm. The ignition data were measured in a shock tube based on sidewall ignition measurements.

Interest in the saturated furans, tetrahydrofurans, has also led to a number of ignition studies of their representatives [22,152,157,196]. One of the studies focusing on this class of biofuels is the study by Dagaut et al. [196], who performed ignition delay time measurements of THF in a single-pulse shock tube, at temperatures of 800–1800 K, pressures of 2–10 atm and equivalence ratios of 0.5–2.0. Based on the shock tube ignition data, they proposed an overall correlation for the relationship of ignition delay time with the mole fractions of all mixture components. Later on, Uygun et al. [22] used a high pressure shock tube to perform ignition delay time measurements for stoichiometric THF/air mixtures at pressures of 20 and 40 bar and temperature ranges of 780–1100 K and 691–1006 K, respectively. The results revealed a two-stage ignition behavior of THF/air mixtures. Moreover, ignition delay times of stoichiometric THF/O_2/inert mixtures were measured by Vanhove et al. [152] in a rapid compression machine at pressures of 0.5–1.0 MPa and temperatures of 640–900 K. The results highlighted a two-stage ignition behavior for temperatures up to 810 K. Ignition delay time exhibited non-Arrhenius dependence on temperature a temperatures between 680 and 750 K. Another study of 2-MTHF ignition was by Fenard et al. [157], who used an RCM to measure ignition delay times of stoichiometric 2-MTHF/O_2/inert mixtures at top dead center pressures of 0.3–2.1 MPa and temperatures of 640–900 K. The main observation was that a two-stage ignition behavior is observed for a temperature range of 685–790 K, which leads to a non-Arrhenius dependence of ignition delay on temperature.

It can be observed that the measurement of ignition delay times of individual furans has been an important research aspect with regards to this class of fuels. While the number of ignition investigations of furans is increasing, few studies focus on structure-activity trends. Studies involving comparative ignition trends between various fuels are discussed next.

4.2.2. Comparative Ignition Studies of Furans

Investigation of comparative ignition behavior is necessary to be able to establish relative reactivity trends. This in turn enables deeper insight into the combustion behavior of furans and further supports chemical kinetic modeling. The following discussion focuses on efforts aimed at comparing the ignition behavior of various furans, as well as comparing furans with pure conventional fuels and blends.

A number of studies focused on comparative reactivity trends among furans and alkyl furans through ignition delay time measurements [24,25,197–200]. One of the leading efforts in this direction was a study by Eldeeb and Akih-Kumgeh [24], which systematically investigated the ignition behavior of furan, 2-MF and 2,5-DMF. Measurements of ignition delay times were performed in a shock tube for fuel/O_2/Ar mixtures over a temperature range of 977–1570 K, pressures of 2–12 atm and equivalence ratios of 0.5–2.0. At fixed pressure, ϕ and D, the results showed that 2,5-DMF exhibited the longest ignition delay times among the three furans and 2-MF had the shortest ignition delay times, with furan showing intermediate behavior, as shown in Figure 8. Increasing the equivalence ratio had a negative effect on ignition delay times, except for 2,5-DMF. Reasonable agreement was observed with literature ignition data [9,10,21], with some disparities that the authors attributed to differences between endwall and sidewall ignition measurements. Another effort by Eldeeb and Akih-Kumgeh [25] involved the investigation of the comparative ignition behavior between 2,5-DMF and 2-ethylfuran (2-EF). The results of 2,5-DMF and 2-EF ignition delay time measurements revealed much shorter ignition delay times for 2-EF, and therefore, 2,5-DMF was established as the

least reactive furan, combining these results with the result of a previous study [24]. Moreover, the findings indicate a universal reactivity behavior between dimethyl and ethyl isomers of cyclic compounds, based on the results of another study by Eldeeb and Akih-Kumgeh [197] that compared the ignition delay times of 2,5-DMF and 2-EF, along with another reactivity trend comparison between 1,3-dimethylcyclohexane and ethylcyclohexane, which revealed a similar trend. The same behavior was previously observed for 1,3-dimethylbenzene (m-xylene) and ethylbenzene by Shen and Oehlschlaeger [201]. Further comparative ignition trends of 2,5-DMF, 2-MF and furan were also studied by Xu et al. [198]. Ignition delay times were measured for 2,5-DMF/Ar/O_2 mixtures at pressures of 1.2–16 bar and temperatures of 1150–2010 K for rich, stoichiometric and lean conditions. Ignition delay times for similar mixtures of 2-MF and furan were measured at stoichiometric conditions. The results indicated that furan exhibited the longest ignition delay times under the investigated conditions. Moreover, the results revealed a strong temperature dependence for the ignition delay times of 2,5-DMF and 2-MF. Xu et al. [199] also compared the auto-ignition behavior of 2,5-DMF and 2-MF at pressures of 16 and 30 bar, temperatures of 737–1143 K and stoichiometric conditions. The results indicated that 2,5-DMF and 2-MF exhibited similar reactivity in the low to intermediate temperature range, with 2-MF being more sensitive to temperature. However, 2,5-DMF exhibited a slightly higher reactivity than 2-MF at temperatures below 925 K. Xu et al. [200] also measured ignition delay times of 2-EF at the same pressure and equivalence ratio conditions and temperatures of 766–1013 K in a rapid compression machine. The ignition delay times of 2-EF were compared to those of 2-MF and 2,5-DMF from the previous study [199], indicating that the relative reactivity trends depends in a complicated way on equivalence ratio and temperature. However, 2-EF was observed to be consistently the most reactive among the three investigated furans.

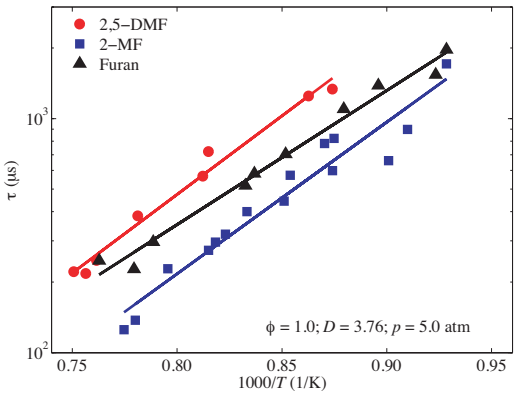

Figure 8. Comparative ignition behavior of furan, 2-MF and 2,5-DMF as shown in Eldeeb and Akih-Kumgeh [24] at a pressure of 5.0 atm, stoichiometric conditions and an Ar/O_2 ratio, *D*, of 3.76.

Relative auto-ignition behavior of tetrahydrofurans was also investigated and compared with alkyl furans in a number of studies [29,202–204]. 2-MTHF auto-ignition behavior received attention for the first time in a study by Wang et al. [202] where high temperature ignition delays of 2-MTHF/O_2/Ar mixtures were measured at pressures of 1.2–10 atm, temperatures of 1050–1800 K, equivalence ratios of 0.5–2.0 and fuel concentrations of 0.25–1.0%. Ignition delay times of 2-MTHF were then compared with those for THF at the same conditions. The results revealed that 2-MTHF has lower ignition delays, and therefore more reactive, than THF. The 2-MTHF ignition delay times were also compared with those for 2-MF in another study by Wang et al. [203], indicating that 2-MF has shorter ignition delay times than 2-MTHF at the same conditions, and therefore, 2-MTHF exhibited lower reactivity that 2-MF, with less pronounced disparities observed at higher temperatures. Moreover, a comparative ignition study of 2-MF and 2-MTHF mixtures with oxygen and argon was performed in a shock tube by Jouzdani et al [29] at equivalence ratios of 0.5–2.0, pressures of 3 and 12 atm and temperatures of 1060–1300 K. 2-MTHF exhibited longer ignition delay times than 2-MF at 3 atm and for lean and

stoichiometric conditions at 12 atm. At rich conditions, the same trend was observed at temperatures above 1075 K, where a cross-over occurs. The authors attributed the overall increased reactivity of 2-MF to its weaker C–H bond sites, which are more sensible to attacks by radicals than in 2-MTHF. It was also indicated that increasing equivalence ratio has a negative effect on ignition delay times. The most extensive comparative study to date of furan, alkyl furans and tetrahydrofurans was presented by Sudholt et al. [204]. Ignition delay times of the furans 2-MF, 2-EF, 2-butylfuran (2-BF) and furan, as well as the tetrahydrofurans THF, 2-MTHF, 3-MTHF and 2-ethyltetrahydrofuran (2-ETHF) were measured in a RCM at stoichiometric conditions and a pressure of 20 bar. The main finding was that the reactivity of the alkyl furans increases with side chain length, while 2-BF exhibited a negative temperature coefficient (NTC). Similarly, side chain location and length were observed to have a significant effect on the reactivity of alkyl tetrahydrofurans.

Other research efforts focused on the ignition behavior of another group of furans, dihydrofurans and established comparative ignition trends of such fuels with other furans [205,206]. Fan et al. [205] measured ignition delay times of 2,3-dihydrofuran (2,3-DHF) and 2,5-dihydrofuran (2,5-DHF) mixtures with oxygen and argon in a shock tube for pressures of 1.2–10 atm, temperatures of 1100–1635 K and equivalence ratios of 0.5–2.0. The ignition delay time data was compared with literature furan data [23,198] to explore the impact of carbon double bonds on ignition behavior. The results revealed that 2,3-DHF exhibited shorter ignition delay times than 2,5-DHF, while furan was observed to have the longest ignition delay times, which was attributed to the stronger bond dissociation energies of furan. In another study by Fan et al. [206], ignition delay times of 2,5-DHF were measured in a shock tube at pressures of 4 and 10 atm, temperatures of 1110–1650 K, equivalence ratios of 0.5 and 1.0 and a fuel concentration of 0.5%. The 2,5-DHF ignition data were further compared to literature furan and 2-MTHF ignition delay times. The comparison revealed that 2,5-DHF has shorter ignition delay times than furan, while it also has shorter ignition delay times than 2-MTHF at lower temperatures, with a cross-over effect occurring around 1400 K and 1460 K at 4 and 10 atm, respectively.

There has also been interest in investigating the relative ignition behavior of furans compared to that of other conventional and bio-derived fuels, as well as blends of furans with other fuels, to further assess their potential as practical fuels or additives [25,199,207]. Eldeeb and Akih-Kumgeh [25] measured ignition delay times of 2,5-DMF and *iso*-octane in a shock tube for temperatures of 1009–1392 K, pressures up to 12 atm and equivalence ratios of 0.5–2.0. It was observed that 2,5-DMF exhibits longer ignition delay times than *iso*-octane. Further ignition delay time measurements of a 2,5-DMF/*iso*-octane 50% blend (by volume) exhibited intermediate reactivity. Later on, Tanaka et al. [207] measured the ignition delay times of 2,5-DMF, 2,5-DMF-PRF90 blends and ethanol-PRF90 blends in a rapid compression machine at temperatures of 692–930 K and pressures of 2.14–2.76 MPa, at stoichiometric conditions and an oxygen concentration of 16.4%. The results indicated that 2,5-DMF is less reactive than gasoline, but more reactive than ethanol. The DMF-PRF90 blend had ignition delay times that are longer than pure PRF90 but shorter than 2-MF-PRF90 blends and ethanol-PRF90 blends. Furthermore, ignition delay times of 2,5-DMF and primary reference fuel (PRF) components such as *n*-heptane, *iso*-octane and toluene were compared by Xu et al. [199]. The results revealed that 2,5-DMF has higher reactivity than toluene, similar reactivity to *iso*-octane and *n*-butanol and much lower reactivity than *n*-heptane and dimethyl ether, indicating the suitability of 2,5-DMF for use in SI engines.

The previous studies have established the relative reactivity trends among a number of furans and tetrahydrofurans, as well as their blends with conventional and bio-derived fuels, which is essential for better understanding of reaction kinetics and model development. The next series of studies focus on flame properties of furans, especially laminar burning velocities.

4.3. Laminar Burning Velocities of Furans

Laminar burning velocities are not only an important combustion characteristic, but they are also useful for the validation of kinetic mechanisms. Laminar burning velocities combine the effects of

reactivity, thermochemical and transport properties. They also serve as a representative for the burning rate in internal combustion engines, which is an important parameter in turbulent simulations [32]. Markstein lengths are also important as they represent thermal-diffusional flame instabilities, which in turn indicate the level of variation between thermal and mass diffusivities in burnt and unburnt regions [32]. The following studies are focused on the characterization of laminar burning velocities and Markstein lengths of different furans [208]. Some of the flame studies focused on the flame characteristics of pure furans such as 2-MF and 2,5-DMF individually, while others investigated the behavior of blends of furans with gasoline surrogates. Furthermore, a group of studies sought to establish comparative flame behavior of various furans.

The flame characterization of pure 2-MF was the target of a number of studies [23,209]. One of the earliest flame studies of 2-MF was a study by Wei et al. [23], who employed tunable synchrotron VUV photoionization along with molecular beam mass spectrometry to study low-pressure premixed laminar 2-MF/O_2/Ar flames at an equivalence ratio range of 0.8–1.5. The authors measured ionization energies (IEs) from photoionization efficiency curves (PIEs) and then compared the measured IEs with literature and calculated values to identify combustion intermediates. The results indicated that H abstraction is the main reaction pathway for 2-MF, based on the identification of species including (Z)-1-oxo-1,3,4-pentatriene, furfural, 2-EF and 2-vinylfuran. Furthermore, OH-addition on the furan ring was identified as an important channel, as 2-oxo-2,3-dihydrofuran was detected. The flame structure of low-pressure 2-MF/O_2/Ar laminar premixed flames was investigated by Cheng et al. [209] at equivalence ratios of 0.80–1.50 using Synchrotron VUV photoionization mass spectrometry. The results identified some of the key species, including 1-oxo-1,3,4-pentatriene, acrolein, 2-furylmethyl, propargyl, 1-oxo-1,3-butadiene and methyl vinyl ketone. Based on the previous results, the authors modified the 2-MF model presented by Somers et al. [11] by adding the formation and consumption reactions of the key species identified, and the modified model was employed to explore the 2-MF reaction pathways. The mechanism was observed to properly predict the H-addition products of 2-MF, but OH-addition products of 2-MF were over-predicted.

Blends of 2-MF with gasoline surrogates captured some research attention as well [210,211]. Ma et al. [210] presented a study that focused on the investigation of laminar burning characteristics of 2-MF/*iso*-octane blends, namely MF20 (20% 2-MF and 80% *iso*-octane) and MF50 (50% 2-MF and 50% *iso*-octane) at temperatures of 333 K, 363 K and 393 K, an initial pressure of 0.1 MPa and equivalence ratios of 0.8–1.4. The results revealed that the laminar burning velocities and unstretched flame speeds of both blends fall between those of the pure fuels. Moreover, maximum un-stretched flame speeds of both blends were observed at equivalence ratios of 1.1–1.2, similar to 2-MF, while Markstein lengths were closer to *iso*-octane at equivalence ratios below 1.2. M50 was observed to have similar burning velocities the average values for 2-MF and *iso*-octane at 393 K. At higher temperatures, the burning velocity behavior for the blend becomes closer to 2-MF. Another study by Tao et al. [211] focused on the effect of initial relative pressure and mix proportion on the flame properties of 2-MF/gasoline blends of 2-MF fractions of 10–50% in a constant-volume napalm bomb. The results revealed that laminar flame speed and critical flame radius were observed to decrease as the ambient pressure increases, while the flame became more unstable. The addition of more 2-MF in the blend led to faster laminar flame propagation speed, smaller unstable critical flame radius and higher flame instability.

Pure 2,5-DMF has also been the focus of numerous flame characterization studies [212–218]. One of the earliest efforts with regards to flame investigation is the study by Wu et al. [212], where a premixed laminar 2,5-DMF/O_2/Ar flame at a pressure of 4 kPa and an equivalence ratio of 2.0 was investigated with tunable synchrotron VUV photoionization coupled with molecular-beam mass spectrometry. The process resulted in the identification of 70 species such as furan and furan-based species, free radicals and aromatics. Therefore, it was proposed that 2,5-DMF consumption takes place by H-abstraction and pyrolysis reactions, while 2-MF and furan are mainly consumed by H-addition, H-abstraction and pyrolysis reactions. The same group measured laminar burning velocities and Markstein numbers of 2,5-DMF premixed outwardly-propagating spherical flames with air-N_2/CO_2

at 1 atm, an initial temperature of 393 K, dilution ratios of 0–15% and equivalence ratios of 0.9–1.5 using high-speed Schlieren photography system [213]. Laminar burning velocity and unstretched flame propagation speed and were both observed to decrease as dilution ratio increases, unlike Markstein length which increased with increasing dilution ratio. As a result, it was indicated that increasing the dilution ratio better stabilizes the flame, with CO_2 as diluent exhibiting stronger effect on flame propagation and stability than N_2. Wu et al. [214] further investigated the effect of pressure on laminar burning velocities of spherically expanding flames of 2,5-DMF/air mixtures at pressures of 0.1–0.75 MPa. The results indicated that increasing the initial pressure leads to decreasing laminar burning velocities and length, which the authors attributed to the increased free-stream density and the increased importance of three-body termination reactions. On the other hand, laminar burning flux was observed to increase with increasing initial pressure. Flame instabilities were found to increase with higher equivalence ratio and initial pressures. Wu et al. [215] also investigated the effect of initial temperature on the laminar burning velocities of 2,5-DMF/air mixtures at 1 atm and initial temperatures of 393 K, 433 K and 473 K. Maximum laminar burning velocity and unstretched flame propagation speed were both observed near the equivalence ratio of 1.2, while they both increased with increasing initial temperature. Tian et al. [216] investigated the laminar flame velocities and Markstein lengths in a constant volume vessel for 2,5-DMF fuel mixtures at equivalence ratios of 0.6–2.0 and initial temperatures of 323–373 K and then compared to EN228 gasoline and ethanol. The results revealed that ethanol has the highest laminar burning velocities, then gasoline and, finally, 2,5-DMF. However, the laminar burning velocities of 2,5-DMF and gasoline were very close to each other in the equivalence ratio range of 0.9–1.1, with differences within 10%. In a study by Wei et al. [217], 2,5-DMF/O_2/Ar low-pressure premixed laminar flames were studied at equivalence ratios of 0.8 and 1.5 to identify the primary combustion intermediates and, therefore, propose possible reaction pathways. The results indicated that H-abstraction was proposed as the main reaction pathway, based on the identified intermediates such as (Z)-1-oxo-1,3,4-pentatriene, 5-methylfurfural and 2-ethyl-5-methylfuran. The study proposed H and OH addition as possible pathways, based on identified species such as (2Z,3E)-1-oxo-1,3-pentadiene, 2-MF and 2-oxo-2,3-dihydro-5-methylfuran. Moreover, the authors hypothesized that the lower laminar burning velocity of 2,5-DMF compared with that of 2-MF is linked to the extra methyl side chain. Liu et al. [218] presented another investigation of 2,5-DMF/O_2/Ar flames at a low pressure of 30 Torr and equivalence ratios of 1.0 and 1.5. The study quantified the mole fractions of major species such as 2-(5-methyl)furylmethyl radical, 1-oxo-1,3,4-pentatriene, 2,5-dimethylene-2,5-dihydrofuran, 2-furylmethyl and cyclopentadienyl radicals and fulvene. The mole fractions were used to modify the 2,5-DMF model by Somers et al. [9]. The modifications included the addition of the fulvene related reactions and the revision of the 2,5-dimethylene-2,5-dihydrofuran reaction kinetics.

A different aspect in 2,5-DMF flame behavior was investigated in a number of studies focused on emission behavior [219,220]. In a study by Gogoi et al. [219], the sooting behavior was investigated for a diffusion flame of 2,5-DMF/diesel blends with up to 15% 2,5-DMF by volume. The results indicated that the addition of more 2,5-DMF in the blends led to reduction in soot emissions and an increase in soot particle reactivity, since the activation energy required for oxidation is much lower than that for the soot emitted from pure diesel. The authors attributed this increase in soot reactivity to the changes in the properties of soot nanostructures. The experimental results revealed that the particle sizes decrease as 2,5-DMF concentration in diesel increases, while an increase in the oxygenated functional groups and the aliphatic character was observed. In a study by Russo et al. [220], the formation tendency of PM in 2,5-DMF mixtures with ethylene was investigated to reveal the impact of fuel-borne oxygen on chemical functionalities and soot nanostructure. The results revealed that the amount of PM produced in the ethylene/2,5-DMF flame is much lower than that produced in pure ethylene flame. However, 2,5-DMF addition to ethylene had a minimal impact of the aromatization of carbon particulate. Moreover, the results from infrared spectrum of the blend flame particles revealed low peaks of aromatic hydrogen

and a high absorption over wavenumbers of 1300–1100 cm^{-1}, which the authors attributed to an increased amount of O atoms replacing H atoms at the edges of ethylene/2,5-DMF soot particles.

The flame characteristics of 2,5-DMF blends with gasoline surrogates were also studied [221,222]. Li et al. [221] investigated laminar flame characteristics of 2,5-DMF/*iso*-octane/air/diluent (15% N_2/85% CO_2) mixtures at an initial temperature of 393 K and atmospheric pressure. The results indicated that laminar flame speeds exhibited little variation with increasing 2,5-DMF concentration, while flame instability slightly increased. Flame front shape revealed an improved flame stability as a result of increasing dilution ratio at fixed equivalence ratio. Moreover, the normalized laminar flame speed was observed to vary linearly with the dilution ratio. Wu et al. [222] also investigated flame characteristics of an 20%/80% 2,5-DMF/*iso*-octane/Air mixture (D20) mixtures at initial temperatures of 393 K, 433 K and 473 K, equivalence ratios of 0.9–1.5 and initial pressures of 0.1–0.5 MPa. The results indicated that Markstein numbers and laminar burning velocities of D20-air are functions of initial temperatures and pressures. Furthermore, it was observed that the flame front cellular structures occur at higher initial pressures, as a result of hydrodynamic and diffusional-thermal instabilities. At equivalence ratios above 1.2, D20-air mixtures exhibited higher laminar burning velocities than *iso*-octane/air mixtures.

The characterization of flame behavior of tetrahydrofurans was also carried out in a few studies [146,223]. Recently, the first effort on 2-MTHF flames was presented by De Bruycker et al. [146], who measured mole fraction profiles of some stable species in 2-MTHF/air premixed flat flames at a pressure of 6.7 kPa and equivalence ratios of 0.7–1.3, as well as laminar burning velocities of flat flames of 2-MTHF/air at initial temperatures of 298–398 K and equivalence ratios of 0.6–1.6, as shown in Figure 9. The results revealed a higher number of detected oxygenates in flames, possibly because of the presence of molecular O_2. The 2-MTHF laminar burning velocities were observed to be lower than those for other saturated and unsaturated cyclic ethers. Based on the previous results as well as those for pyrolysis experiments performed in the same study, the authors developed a kinetic model for combustion and pyrolysis simulations of 2-MTHF, which slightly over-predicted laminar burning velocities. Moreover, a recent study by Jiang et al. [223] focused on investigation of laminar burning characteristics of 2-MTHF/air mixtures at equivalent ratios of 0.88–1.43, initial temperatures of 333 K, 363 K and 393 K and atmospheric pressure in a constant-volume vessel. The study results were further compared with those for ethanol and *iso*-octane. The result revealed that ethanol generally exhibits the fastest un-stretched flame propagation speed, *iso*-octane has the slowest propagation speeds, while 2-MTHF shows intermediate behavior. The un-stretched flame speeds were observed to be maximum at equivalence ratios of 1.1–1.2 for all fuels. Based on Markstein length results, *iso*-octane was observed to be more stable flame than 2-MTHF and ethanol equivalence ratio of 1.2 at 393 K. Moreover, the smallest flame thickness was generally observed in the case of ethanol. In terms of laminar burning velocities, 2-MTHF has much faster flames than those for *iso*-octane, but similar to those of ethanol. The results highlighted the fast-burning of 2-MTHF, which makes it promising in terms of enhancing engine thermal efficiency.

Another group of flame studies included comparative flame characterization between furans [224–228]. High-speed Schlieren photography was used by Ma et al. [224] in constant-volume vessel to investigate laminar flame characteristics of 2-MF/air mixtures at temperatures of 333–393 K, equivalence ratios of 0.6–1.1 and an initial pressure of 0.1 MPa. The results indicated that at higher stretch rates, faster stretched flame propagation speeds of 2-MF were observed. Moreover, 2-MF was observed to exhibit unstretched flame speeds up to 30% faster than 2,5-DMF and up to 50% faster than *iso*-octane. 2-MF was observed to be similar to 2,5-DMF, as their maximum unstretched flame speeds were observed at the same equivalence ratio of 1.1, while that for *iso*-octane was observed at an equivalence ratio of 1.2. Markstein lengths and flame thickness of 2-MF were observed to be smaller than those of 2,5-DMF and *iso*-octane in general, while 2-MF exhibited the fastest burning velocity at all conditions. In another study by Gillespie [225], a flat-flame burner was used to measure Laminar burning velocities of 2-MF/air mixtures at a pressure of 1.0 atm, temperatures of

298–398 K and equivalence ratios of 0.55–1.65. It was observed that burning velocities increase at higher temperatures, with the maximum burning velocities at an equivalence ratio of 1.1. Moreover, burning velocities of 2,5-DMF/air mixtures were measured at 1 atm, temperatures of 298 and 358 K and equivalence ratios of 0.60–1.60, which indicated similar temperature dependence and maximum burning velocity conditions to 2-MF. The results for both fuels were compared, revealing that 2-MF exhibits laminar burning velocities which are about 18 cm/s faster than those of 2,5-DMF at an equivalence ratio of 1.1. Tran et al. [226] measured the laminar premixed flame structure of 2,5-DMF and 2-MF at rich conditions and low pressure (40 kPa) using sampling by a sonic probe then gas chromatography. The results quantified the mole fraction profiles numerous 31 and 40 products and intermediates for 2-MF and 2,5-DMF, respectively, including heavy aromatics such as ethylbenzene and styrene. The results indicated that the production of heavy aromatics is higher in the case of 2,5-DMF than 2-MF. The results were used to update a 2,5-DMF and 2-MF kinetic model with new reactions for C8 aromatics as well as large Polycyclic Aromatic Hydrocarbons (PAH) formation. In another study by Sirignano et al. [227], counter-flow diffusion flames of 2-MF, 2,5-DMF and furan were investigated using optical techniques such as Laser Induced Fluorescence and Incandescence, in order to identify small nanoparticles and soot aggregates. Experimental results indicated that particle production was increased in furan-based fuels, with furan exhibiting the lowest particle production among the three furans. Moreover, 2-MF was observed to produce more particles than 2,5-DMF; both producing more particles than furan. Further, the particulate matter (PM) formation tendency of the three fuels was investigated by the same group [228] for premixed flames of mixtures of the three fuels with ethylene at 1 atm and equivalence ratios of 2.01–2.46. Laser UV-induced emission was used for the detection of precursor nanoparticles, through the changing of the wavelength from the UV to the visible. As furans were added to the mixture, both UV and VIS signals were observed to slightly decrease, indicating a minimal impact on small particle formation. Moreover, Laser Induced Incandescence (LII) was employed to detect soot particles, and the LII signals were observed to decrease significantly as furans are added, indicating a significant impact on soot formation.

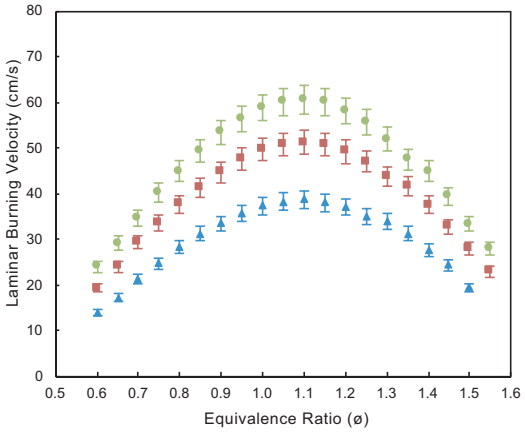

Figure 9. Laminar burning velocities for flames of MTHF/air mixtures at 0.101 MPa. Circles: $T_{gas,unburned}$ = 298 K, squares: $T_{gas,unburned}$ = 358 K, triangles: $T_{gas,unburned}$ = 398 K (adapted from De Bruycker et al. [146]).

In summary of this section, various studies that characterized different combustion properties of furans were reviewed. These properties included engine performance, emission levels, ignition behavior, comparative reactivity trends, as well as laminar burning characteristics. The body of literature in this research direction provided indispensable amount of data that are used to map the combustion behavior of such fuels at a wide range of conditions. This is crucial for the development of chemical kinetic models used for the simulation of such combustion behavior. In the coming section,

the work done on the validation of proposed chemical kinetic models of furans will be discussed. The studies above include these validations but this section focuses on the validation part.

5. Validation of Proposed Chemical Kinetic Models

So far, the development process of detailed chemical kinetic mechanisms is not yet mature or advanced to depend on theory alone. As a result, it still relies on experimental data of key combustion properties, which are used as validation targets of proposed models. This section sheds some light on studies aimed at the validation of proposed chemical kinetic models of furans, by comparing the model predictions of fundamental combustion properties such as laminar burning velocities and ignition delay times with experimental observations. Validation studies are grouped in this section into models of individual furans and combined models.

Model validations of furan models have been carried out. One of the earliest studies is the study by Wei et al. [23], where ignition delay time measurements at 1.2 atm were used for the validation of a furan kinetic mechanism (Mech FR) by Tian et al. [8]. The results showed reasonable agreement between experiments and model predictions at rich conditions. However, serious deviations were observed at stoichiometric and lean conditions, where the model significantly under predicts ignition delay times, especially at temperatures below 1667 K. Based on sensitivity analysis, the rate constants of the most relevant reactions were adjusted to develop a modified version of Mech FR. Significantly improved performance was observed in modified model predictions of ignition delay times and pyrolysis product concentration profiles. Results from the modified version revealed the most important channel for furan consumption, which is the initiation reaction: furan $\rightarrow$ formyl allene ($CH_2CCHCHO$), rather than the H abstraction reactions proposed by the original Mech FR.

2-MF was the target for a number of model validation studies [21,141,209]. In a study by Wei et al. [21], The 2-MF model NUI_MF2 by Somers et al. [11] was validated against ignition delay time measurements of 2-MF. The model predicted the ignition delay times of 2-MF with reasonable accuracy at 1.25 bar, but under-predicted the ignition delay times at pressures of 4.25 and 10.65 bar. The reactions containing the *n*-butadienyl radical (C_4H_5-*n*) were identified by sensitivity analysis as important channels during the ignition of 2-MF. Furthermore, the rate constants of β-scission reactions for C_4H_5-*n* were modified, which improved the predictive performance of the model. Moreover, Cheng et al. [141] updated the 2-MF model by Somers et al. [11] for better predictions of aromatic species formation during 2-MF pyrolysis. This was achieved by modifying and expanding the existing aromatic formation sub-mechanism with reactions involving species such as phenylacetylene, indene, indenyl radical and naphthalene. The updated model was validated against concentration profiles measured in a flow reactor. The results revealed that decomposition is the main pathway for 2-MF consumption, which leads to the formation of propargyl and acetyl radicals. At higher fuel concentrations, 2-MF exhibited higher aromatics formation than 2,5-DMF during pyrolysis, due to the high concentration of propargyl radical, a precursor of aromatics. Another modification to the 2-MF model by Somers et al. [11] was presented by Cheng et al. [209] for the purpose of modeling 2-MF pyrolysis and flame characteristics. The modification included updating and incorporating some key reactions such as the isomerization reactions of fulvene, the recombination reactions of C_3H_3 and the H-addition reactions of propenal, a product of OH-addition pathway. The simulation results indicated that the H-addition products of 2-MF such as furan and 1-oxo-1,3-butadiene were properly predicted, while the concentrations of H-abstraction products of 2-MF such as 1-oxo-1,3,4-pentatriene and 2-furylmethyl were under-predicted. The model was observed to over-predict the concentrations of acrolein, an OH-addition product of 2-MF.

Moreover, several studies focused on the validation of 2,5-DMF models [20,144,145,199,218,229]. A study by Saggese et al. [229] presented a lumped kinetic model (~400 species, 10,000 reactions) for pyrolysis of furans. The model predictions were compared to literature concentration profiles and ignition delay times, indicating reasonable agreement between predicted 2,5-DMF conversion rates and experimental data by Lifshitz et al. [142]. However, the model under-predicted the 2,5-DMF conversion

rate compared to the experimental data of Djokic et al. [143]. Furthermore, Alexandrino et al. [20,144] validated their 2,5-DMF model [144] against concentration measurements obtained in a flow reactor for 2,5-DMF in the presence and the absence of nitric oxide. The model was based on the model by Sirjean et al. [10], with a 2,5-DMF subset added to reach a final version of 255 species and 1314 reactions. Reasonable agreement was observed between experimental data and model predictions. In another study by Liu et al. [218], a modified 2,5-DMF model was developed through the addition of the fulvene kinetics to the Somers model [9] and the development of the 2,5-dimethylene-2,5-dihydrofuran reaction kinetics. The concentration profiles obtained experimentally from a laminar premixed flame of 2,5-DMF/O_2/Ar were compared to predictions of the modified model, Somers model and Togbé model [161]. Somers model and the revised model were observed to reasonably predict the maximum mole fraction of DMF252J, which was over-predicted by the Togbé model. The peak mole fraction of 2-MF was well predicted by the revised model at rich conditions, but over-predicted by all models at other conditions. Moreover, the revised model well-predicted the concentration profiles of fulvene while over-predicting those of benzene. Furthermore, Alexandrino et al. [145] used their experimentally obtained soot and light gas concentrations of 2,5-DMF pyrolysis in a flow reactor to validate their 2,5-DMF chemical kinetic model [144]. Poor quantitative agreement was observed between the experimental data and model predictions, due to the lack of soot formation reactions in the model, except for a naphthalene sub-mechanism. However, the model qualitatively captured the experimental trends, except for acetylene. The RCM ignition delay data of 2,5-DMF by Xu et al. [199] were used to validate the 2,5-DMF models by Somers et al. [9] and Liu et al. [159]. The predictions of both models exhibited some deviation from the experimental data, with the model by Somers et al. [9] showing relatively better performance. Therefore, the rate constants of 10 H-abstraction reactions in the model of Somers et al. [9] were modified. Moreover, the rate constant of the reaction DMF252J + HO_2 → DMF252OJ + OH was reduced by a factor of 1.5. As a result, the modified model exhibited better qualitative and quantitative predictive performance of 2,5-DMF ignition behavior. Reaction pathway analysis showed similarity in the consumption pathways for 2,5-DMF and 2-MF, through H-abstraction, H radical release, disproportionation and subsequent decomposition reactions.

Other alkyl furans, such as 2-EF, received some attention with regards to model validation. Ignition delay times of 2-EF obtained by Xu et al. [200] were used for the validation of a modified version of the model by Somers et al. [9], which did not include an extensive 2-EF sub-mechanism. The modifications included the incorporation of HO_2 addition reactions for E2F2J-A radical and H abstraction by oxygen reactions for E2F2J-P radical. Moreover, H-abstractions by oxygen, H, OH and CH_3 of V2F were included in the model, as well as reactions of V2FJ-P. The results showed better agreement between the model predictions and the experimental measurements of the study as well as literature ignition delay times of 2-EF [25]. Reaction pathway analysis using the modified model indicated that H-abstraction reactions are the favored channel for 2,5-DMF consumption, since it is more branched. On the other hand, OH-addition reactions at C2 and C5 positions appeared to be the favored pathway for both 2-EF and 2-MF. Despite the similarities between the oxidation kinetics of alkylfurans and alkylbenzenes at low to intermediate temperatures, alkylfurans were observed to undergo OH-addition reactions on the ring, which was not observed in alkylbenzenes.

Furthermore, model validation efforts were carried out for tetrahydrofurans. Wang et al. [203] compared shock tube ignition delay times of 2-MTHF with the predictions of the model by Moshammer et al. [27] (Mech I) and the model by Tran et al. [158] (Mech II). The results revealed that Mech II under-predicted ignition delay times of 2-MTHF, with better agreement observed at lower temperatures. However, Mech I exhibited good agreement with ignition delay times of 2-MTHF, except for temperatures around 1250 K at rich conditions. To further improve the agreement, Mech I was combined with the AramcoMech_1.3 model by Metcalfe et al. [230] to produce a new model (Mech III). The model was observed to reasonably reproduce ignition delay times of 2-MTHF under all investigated conditions.

Model validation studies of dihydrofurans have been also carried out [205,206]. Fan et al. [206] compared their ignition delay time measurement for 2,5-DHF with the predictions of models by Liu et al. [159], Somers et al. [9] and Tran et al. [160]. The results revealed that Liu model exhibited better qualitative and quantitative agreement with the 2,5-DHF ignition delay times, while the Somers model generally under-predicted ignition delay times. The Tran model was unable to capture equivalence ratio and pressure effects on reactivity. As a result, the model by Liu et al. [159] was used to perform reaction pathway and sensitivity analysis, which revealed that the main intermediates in the consumption of 2,5-DHF are allyl radicals and propylene. Another study by Fan et al. [205] used ignition delay times for 2,3-DHF and 2,5-DHF for the validation of the existing chemical kinetic models by Tian et al. [8], Somers et al. [11], Tran et al. [158] and Moshammer et al. [27]. The models exhibited similar predictive accuracy, with poor quantitative prediction for ignition delay times and activation energy of the two DHFs under the investigated conditions, due to the lack of detailed DHF reaction mechanism. As a result, the authors applied several modifications to the model by Tran et al. [158] to improve its predictive accuracy. The modifications included the addition of 2,3-DHF decomposition reactions, as well as rate constant adjustment of some initial H-elimination reactions. Activation energy and ignition delay times predictions using the modified model were significantly improved for both 2,3-DHF and 2,5-DHF over the investigated temperature range (1100–1635 K).

Another group of chemical kinetic model validation studies focused on the validation of models against ignition and concentration data for multiple furans and tetrahydrofurans [24,29,139,155,198,227]. Eldeeb and Akih-Kumgeh [24] used their ignition delay time measurements for 2,5-DMF and 2-MF for comparison with chemical kinetic models by Sirjean et al. [10] and Somers et al. [9]. The comparative reactivity trend was qualitatively captured by both models, indicating that 2,5-DMF is less reactive than 2-MF. The model by Somers et al. [9] was observed to have better quantitative agreement with experimental data, while the other model [10] over-predicted ignition delay times under most conditions. Sirignano et al. [227] added a detailed kinetic mechanism for particulate formation, developed earlier by the same group [231–233], to the model by Somers et al. [11] to produce a new kinetic mechanism for particulate formation during the decomposition of furan, 2-MF and 2,5-DMF. The new model captured the experimentally obtained trend under the experimental conditions of the study, showing that furan has the lowest particle formation propensity, then 2,5-DMF and, finally, 2-MF. The modeling results revealed that large amounts of C4 compounds are produced from 2-MF, which leads to the production of benzene and polycyclic aromatic hydrocarbons (PAHs). Phenol was the main product from 2,5-DMF decomposition, leading to the formation of cyclopentadiene and naphthalene. In a study by Xu et al. [198], ignition delay times for 2,5-DMF, 2-MF and furan were compared to the predictions of the models by Somers et al. [9] and Liu et al. [159]. The results indicated qualitative agreement between the predictions of both models and 2,5-DMF and 2-MF relative ignition trends, with the model of Somers et al. [9] exhibiting better quantitative agreement for both fuels. As a result, rate constant modifications were performed to the Somers model to enhance its quantitative agreement with ignition data of furans. Better agreement was observed as a result, especially at elevated pressures and lower temperatures. Further reaction pathway and sensitivity analyses revealed that H-abstractions from the methyl side become more important for both 2,5-DMF and 2-MF at higher temperatures. However, the process results in the formation of different radicals in both cases, leading to reduced reactivity of 2,5-DMF relative to that of 2-MF. Recently, a study by Cheng et al. [139] used mole fraction profiles obtained from the low-pressure pyrolysis of furan for the validation of a combustion model of furan, 2-MF and 2,5-DMF developed by incorporating the submechanism of furan from the model by Tian et al. [8] into the 2-MF model by Somers et al. [11]. The results revealed that the main decomposition channels of furan go through unimolecular decomposition reactions. The results suggested that propargyl radical is formed through the direct decomposition of propyne rather than that of furan. In another study by Tran et al. [155], the model for furan, 2-MF and 2,5-DMF by Sirjean et al. [10] was extended to include the low-to-moderate temperature (LMT) oxidation kinetics. The model was claimed to include a more extensive description of reactions of fuel

radicals for LMT oxidation than all previously reported chemical kinetic models for furans. The model was validated against the speciation data for the three fuels from the same study, obtained from LMT oxidation in a flow reactor. The results indicated that the conversion rates of 2,5-DMF were the most sensitive to equivalence ratio, with 2-MF and furan exhibiting significantly lower sensitivity. The simulation results revealed that toxic oxygenates such as furfural, acrolein, methyl vinyl ketone and phenol are produced from the primary reaction of the three fuels. Tetrahydrofurans received some attention in a study by Jouzdani et al. [29], where the authors compared ignition delay times of 2-MF and 2-MTHF with the predictions of the 2-MF model by Somers et al. [11] and the 2-MTHF model by Moshammer et al. [27]. The results indicated that both models generally under-predicted ignition delay times relative to the experimental data. Furthermore, concentration time histories of 2-MTHF were measured and compared to model predictions. The comparison results were consistent with the deviation observed in ignition predictions, since the model predictions of 2-MTHF concentration profiles indicated much faster 2-MTHF consumption rate than the actual rate in the experiments.

Recently, the validation of combined models of furans with gasoline surrogates was carried out in a number of studies [25,207]. Eldeeb and Akih-Kumgeh validated their 2,5-DMF/*iso*-octane model [25] against ignition delay times of 2,5-DMF/*iso*-octane blends, as well as literature data by Somers et al. [9] for pure 2,5-DMF. The combined model was observed to capture the qualitative reactivity trends of the blend as well as the pure fuels. The model was observed to perform better than the original model by Somers et al. [9] at higher pressures, as shown in Figure 10. Moreover, in a study by Tanaka et al. [207], RCM ignition delay times of 2,5-DMF, 2,5-DMF/PRF gasoline blends, 2-MF/PRF blends and ethanol/PRF blends were simulated using the 2,5-DMF model by Somers et al. [9], a new DMF-PRF model based on the Somers model and the PRF model by Curran et al. [234]. The new model was unable to properly predict the ignition behavior of ethanol-PRF blends. However, reasonable agreement was observed between simulations and ignition delay times of 2,5-DMF/PRF90 and 2-MF/PRF90 blends.

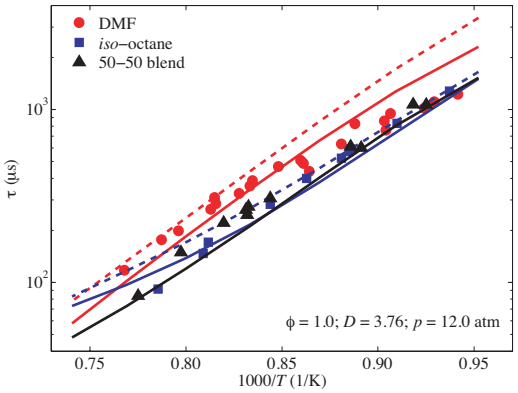

Figure 10. Experimental ignition delay times compared with model predictions for stoichiometric 2,5-DMF, *iso*-octane mixture and 50-50 blends at 12.0 atm, as shown in Eldeeb and Akih-Kumgeh [25]. Solid lines: blend model. Dashed lines: original 2,5-DMF and *iso*-octane models [9,235].

From the previous discussion, it can be suggested that further validation, modification, and the extension of existing models is necessary for better predictions of key reaction and combustion characteristics, ultimately leading to better understanding of the potential of such compounds as biofuel candidates. The next section will feature a summary and some conclusions of this work.

6. Summary and Conclusions

Furans and tetrahydrofurans such as 2,5-DMF, 2-MF, THF, 2-MTHF, and others, are promising second generation bio-derived fuels. This class of fuels is considered a promising candidate for use in both SI and CI engines as pure fuels or fuel extenders. In this review, the production methods of

furanic fuels have been demonstrated in order to put the commercial interest of such fuel in context. Then, the review discusses the vast body of literature focused on the experimental characterization of furan. This is aimed at the exploration of the potential research opportunities with regards to such fuels and therefore advances knowledge, understanding and utilization of furans.

From a production standpoint, HMF and furfural are identified as the most important platform chemicals in the production of furans, especially 2,5-DMF, 2-MF and furan. A wide range of noble and non-noble metallic catalysts were used in the production processes of such fuels from biomass. The production methods of furans have witnessed a significant improvement with respect to conversion rates and yields. However, some problems related to separation, purification and sustainability need to be addressed for these production methods to reach their full potential.

Fundamental combustion characteristics such as laminar flame speeds and structures, ignition delay times and pyrolysis species profiles have been investigated extensively for furan-based fuels. The overall results indicated that 2,5-DMF has similar laminar burning velocities to those of gasoline, with lower velocities than 2-MF, while furan and tetrahydrofurans were not as extensively studied. For ignition delay times of furan-based fuels, 2,5-DMF exhibited lower reactivity than 2-MF and furan in most studies, under low pressure and high temperature conditions. Moreover, the combustion chemistry of furans was explored through a wide range of studies on the oxidation and pyrolysis of furans in flow reactors. The most important finding is that 2,5-DMF produces large quantities of soot precursors, which leads to a sooting propensity in 2,5-DMF flames.

Based on experimental characterizations and quantum chemical calculations, several modeling efforts have been reported, with agreement between most models and experimental validation targets such as ignition delay times being mostly qualitatively, while quantitative agreement was observed in some cases. The quantitative predictive accuracy of chemical kinetic models can only be improved by expending the parameter range of experimental data used for model development, as well as proper quantification and elimination of experimental and numerical uncertainties.

This review indicates that more extensive experimental data on key combustion characteristics are needed for validation of model performance. One possibility is extending concentration measurements of furans and other important species to wider ranges of temperature, pressure and equivalence ratio, which will add constraints to the proposed models, ultimately improving their predictive performance. Species concentration measurements can be performed during shock tube pyrolysis and ignition and can serve as validation targets for chemical kinetic models in addition to ignition delay times. However, it is observed that very few research efforts have exploited this capability of shock tubes. Optical diagnostic techniques, such as mid-infrared laser absorption, laser extinction, laser induced fluorescence and LII, should continue to be employed to measure and record soot concentration time histories and particle characteristics during ignition, pyrolysis, as well as flame propagation of furans, in order to perform proper assessment of the environmental impacts of this class of biofuels with respect to emissions, apart from the established toxicity levels.

Finally, this review highlights the importance of developing analytic expressions and functions that can be used to summarize the performance of given detailed chemical kinetic models. One way is to develop ignition delay correlations from chemical kinetic models simulations over a wide range of conditions. Such correlations would facilitate the prediction of simulated ignition delay times at a wide range of conditions. In summary, this review promotes further experimental and modeling research efforts with the purpose of further enhancement of chemical kinetic model performance for this promising class of fuels.

Acknowledgments: Support from Lyles College of Engineering at California State University, Fresno, and the School of Engineering and Computer Science at Syracuse University is acknowledged.

Author Contributions: Mazen A. Eldeeb collected, organized and analyzed the references and wrote the paper. Benjamin Akih-Kumgeh planned and outlined the review methodology and provided modification suggestions for the manuscript.

Conflicts of Interest: The authors declare no conflict of interest.

References

1. International Energy Agency. *Key World Energy Statistics*; International Energy Agency: Paris, France, 2014.
2. Pachauri, R.K.; Reisinger, A. *Climate Change 2007 Synthesis Report: Summary for Policymakers*; IPCC Secretariat: Geneva, Switzerland, 2007.
3. Román-Leshkov, Y.; Barrett, C.J.; Liu, Z.Y.; Dumesic, J.A. Production of dimethylfuran for liquid fuels from biomass-derived carbohydrates. *Nature* **2007**, *447*, 982–985.
4. Tong, X.; Ma, Y.; Li, Y. Biomass into chemicals: Conversion of sugars to furan derivatives by catalytic processes. *Appl. Catal. A* **2010**, *385*, 1–13.
5. Chidambaram, M.; Bell, A.T. A two-step approach for the catalytic conversion of glucose to 2,5-dimethylfuran in ionic liquids. *Green Chem.* **2010**, *12*, 1253–1262.
6. Mascal, M.; Nikitin, E.B. Direct, High-Yield Conversion of Cellulose into Biofuel. *Angew. Chem. Int. Ed.* **2008**, *120*, 8042–8044.
7. Sanderson, K. Lignocellulose: A chewy problem. *Nature* **2011**, *474*, S12–S14.
8. Tian, Z.; Yuan, T.; Fournet, R.; Glaude, P.A.; Sirjean, B.; Battin-Leclerc, F.; Zhang, K.; Qi, F. An experimental and kinetic investigation of premixed furan/oxygen/argon flames. *Combust. Flame* **2011**, *158*, 756–773.
9. Somers, K.P.; Simmie, J.M.; Gillespie, F.; Conroy, C.; Black, G.; Metcalfe, W.K.; Battin-Leclerc, F.; Dirrenberger, P.; Herbinet, O.; Glaude, P.A.; et al. A comprehensive experimental and detailed chemical kinetic modelling study of 2,5-dimethylfuran pyrolysis and oxidation. *Combust. Flame* **2013**, *160*, 2291–2318.
10. Sirjean, B.; Fournet, R.; Glaude, P.A.; Battin-Leclerc, F.; Wang, W.; Oehlschlaeger, M.A. Shock Tube and Chemical Kinetic Modeling Study of the Oxidation of 2,5-Dimethylfuran. *J. Phys. Chem. A* **2013**, *117*, 1371–1392.
11. Somers, K.; Simmie, J.; Gillespie, F.; Burke, U.; Connolly, J.; Metcalfe, W.; Battin-Leclerc, F.; Dirrenberger, P.; Herbinet, O.; Glaude, P.A.; et al. A high temperature and atmospheric pressure experimental and detailed chemical kinetic modelling study of 2-methyl furan oxidation. *Proc. Combust. Inst.* **2013**, *34*, 225–232.
12. Zhong, S.; Daniel, R.; Xu, H.; Zhang, J.; Turner, D.; Wyszynski, M.L.; Richards, P. Combustion and Emissions of 2,5-Dimethylfuran in a Direct-Injection Spark-Ignition Engine. *Energy Fuels* **2010**, *24*, 2891–2899.
13. Daniel, R.; Xu, H.; Wang, C.; Richardson, D.; Shuai, S. Combustion performance of 2,5-dimethylfuran blends using dual-injection compared to direct-injection in a {SI} engine. *Appl. Energy* **2012**, *98*, 59–68.
14. Rothamer, D.A.; Jennings, J.H. Study of the knocking propensity of 2,5-dimethylfuran-gasoline and ethanol-gasoline blends. *Fuel* **2012**, *98*, 203–212.
15. Gouli, S.; Lois, E.; Stournas, S. Effects of Some Oxygenated Substitutes on Gasoline Properties, Spark Ignition Engine Performance, and Emissions. *Energy Fuels* **1998**, *12*, 918–924.
16. Christensen, E.; Yanowitz, J.; Ratcliff, M.; McCormick, R.L. Renewable oxygenate blending effects on gasoline properties. *Energy Fuels* **2011**, *25*, 4723–4733.
17. Ma, X.; Jiang, C.; Xu, H.; Ding, H.; Shuai, S. Laminar burning characteristics of 2-methylfuran and isooctane blend fuels. *Fuel* **2014**, *116*, 281–291.
18. Pan, M.; Shu, G.; Pan, J.; Wei, H.; Feng, D.; Guo, Y.; Liang, Y. Performance comparison of 2-methylfuran and gasoline on a spark-ignition engine with cooled exhaust gas recirculation. *Fuel* **2014**, *132*, 36–43.
19. Cheng, Z.; Xing, L.; Zeng, M.; Dong, W.; Zhang, F.; Qi, F.; Li, Y. Experimental and kinetic modeling study of 2,5-dimethylfuran pyrolysis at various pressures. *Combust. Flame* **2014**, *161*, 2496–2511.
20. Alexandrino, K.; Millera, A.; Bilbao, R.; Alzueta, M.U. Interaction between 2,5-dimethylfuran and nitric oxide: Experimental and modeling study. *Energy Fuels* **2014**, *28*, 4193–4198.
21. Wei, L.; Tang, C.; Man, X.; Huang, Z. Shock-Tube Experiments and Kinetic Modeling of 2-Methylfuran Ignition at Elevated Pressure. *Energy Fuels* **2013**, *27*, 7809–7816.
22. Uygun, Y.; Ishihara, S.; Olivier, H. A high pressure ignition delay time study of 2-methylfuran and tetrahydrofuran in shock tubes. *Combust. Flame* **2014**, *161*, 2519–2530.
23. Wei, L.; Tang, C.; Man, X.; Jiang, X.; Huang, Z. High-Temperature Ignition Delay Times and Kinetic Study of Furan. *Energy Fuels* **2012**, *26*, 2075–2081.
24. Eldeeb, M.A.; Akih-Kumgeh, B. Reactivity Trends in Furan and Alkyl Furan Combustion. *Energy Fuels* **2014**, *28*, 6618–6626.
25. Eldeeb, M.A.; Akih-Kumgeh, B. Investigation of 2,5-dimethyl furan and iso-octane ignition. *Combust. Flame* **2015**, *162*, 2454–2465.

26. Simmie, J.M. Kinetics and thermochemistry of 2,5-dimethyltetrahydrofuran and related oxolanes: Next next-generation biofuels. *J. Phys. Chem. A* **2012**, *116*, 4528–4538.
27. Moshammer, K.; Vranckx, S.; Chakravarty, H.K.; Parab, P.; Fernandes, R.X.; Kohse-Höinghaus, K. An experimental and kinetic modeling study of 2-methyltetrahydrofuran flames. *Combust. Flame* **2013**, *160*, 2729–2743.
28. Sudholt, A.; Cai, L.; Heyne, J.; Haas, F.M.; Pitsch, H.; Dryer, F.L. Ignition characteristics of a bio-derived class of saturated and unsaturated furans for engine applications. *Proc. Combust. Inst.* **2015**, *35*, 2957–2965.
29. Jouzdani, S.; Eldeeb, M.A.; Zhang, L.; Akih-Kumgeh, B. High-Temperature Study of 2-Methyl Furan and 2-Methyl Tetrahydrofuran Combustion. *Int. J. Chem. Kinet.* **2016**, *48*, 491–503.
30. Aylott, M. Biomass Gasification in the UK—Where are we Now? *Biomass Mag.* **2010**, *4*, 22–26.
31. Leitner, W.; Klankermayer, J.; Pischinger, S.; Pitsch, H.; Kohse-Höinghaus, K. Advanced Biofuels and Beyond: Chemistry Solutions for Propulsion and Production. *Angew. Chem. Int. Ed.* **2017**, *56*, 5412–5452.
32. Xu, N.; Gong, J.; Huang, Z. Review on the production methods and fundamental combustion characteristics of furan derivatives. *Renew. Sustain. Energy Rev.* **2016**, *54*, 1189–1211.
33. Kwon, Y.; Schouten, K.J.P.; van der Waal, J.C.; de Jong, E.; Koper, M.T. Electrocatalytic Conversion of Furanic Compounds. *ACS Catal.* **2016**, *6*, 6704–6717.
34. Yanowitz, J.; Christensen, E.; McCormick, R.L. *Utilization of Renewable Oxygenates as Gasoline Blending Components*; Technical Report; National Renewable Energy Laboratory (NREL): Golden, CO, USA, 2011.
35. Dreyfuss, P. *Poly(Tetrahydrofuran)*; CRC Press: Boca Raton, FL, USA, 1982; Volume 8.
36. Dutta, S.; De, S.; Saha, B.; Alam, M.I. Advances in conversion of hemicellulosic biomass to furfural and upgrading to biofuels. *Catal. Sci. Technol.* **2012**, *2*, 2025–2036.
37. Lange, J.P.; van der Heide, E.; van Buijtenen, J.; Price, R. Furfural—A promising platform for lignocellulosic biofuels. *ChemSusChem* **2012**, *5*, 150–166.
38. Jężak, S.; Dzida, M.; Zorębski, M. High pressure physicochemical properties of 2-methylfuran and 2,5-dimethylfuran—Second generation biofuels. *Fuel* **2016**, *184*, 334–343.
39. Burnett, L.; Johns, I.; Holdren, R.; Hixon, R. Production of 2-methylfuran by vapor-phase hydrogenation of furfural. *Ind. Eng. Chem.* **1948**, *40*, 502–505.
40. Sun, Q.; Liu, S.F.; Yao, X.H.; Su, Y.C.; Zhang, Z. Catalytic Study on Hydrogenation of Carbonyl Group into Methylene or Methyl Group by Silica-supported Poly(acrylonitrile-vinyltriethoxysilicon) Palladium (II) Complex. *Chin. J. Synth. Chem.* **1996**, *4*, 146–150.
41. Rao, R.S.; Baker, R.T.K.; Vannice, M.A. Furfural hydrogenation over carbon-supported copper. *Catal. Lett.* **1999**, *60*, 51–57.
42. Zheng, H.Y.; Zhu, Y.L.; Teng, B.T.; Bai, Z.Q.; Zhang, C.H.; Xiang, H.W.; Li, Y.W. Towards understanding the reaction pathway in vapour phase hydrogenation of furfural to 2-methylfuran. *J. Mol. Catal. A Chem.* **2006**, *246*, 18–23.
43. Li, C.; Li, G. A new orbital complex catalyst for vapor phase hydrogenation of furfural to 2-methylfuran. *Ind. Catal.* **2008**, *16*, 60–64.
44. Sitthisa, S.; An, W.; Resasco, D.E. Selective conversion of furfural to methylfuran over silica-supported Ni Fe bimetallic catalysts. *J. Catal.* **2011**, *284*, 90–101.
45. Zhang, J.; Lin, L.; Liu, S. Efficient Production of Furan Derivatives from a Sugar Mixture by Catalytic Process. *Energy Fuels* **2012**, *26*, 4560–4567.
46. Nilges, P.; Schröder, U. Electrochemistry for biofuel generation: Production of furans by electrocatalytic hydrogenation of furfurals. *Energy Environ. Sci.* **2013**, *6*, 2925–2931.
47. Dong, F.; Zhu, Y.; Zheng, H.; Zhu, Y.; Li, X.; Li, Y. Cr-free Cu-catalysts for the selective hydrogenation of biomass-derived furfural to 2-methylfuran: The synergistic effect of metal and acid sites. *J. Mol. Catal. A Chem.* **2015**, *398*, 140–148.
48. Dong, F.; Ding, G.; Zheng, H.; Xiang, X.; Chen, L.; Zhu, Y.; Li, Y. Highly dispersed Cu nanoparticles as an efficient catalyst for the synthesis of the biofuel 2-methylfuran. *Catal. Sci. Technol.* **2016**, *6*, 767–779.
49. Zhu, Y.L.; Xiang, H.W.; Li, Y.W.; Jiao, H.; Wu, G.S.; Zhong, B.; Guo, G.Q. A new strategy for the efficient synthesis of 2-methylfuran and γ-butyrolactone. *New J. Chem.* **2003**, *27*, 208–210.
50. Zheng, H.Y.; Zhu, Y.L.; Bai, Z.Q.; Huang, L.; Xiang, H.W.; Li, Y.W. An environmentally benign process for the efficient synthesis of cyclohexanone and 2-methylfuran. *Green Chem.* **2006**, *8*, 107–109.

51. Zheng, H.Y.; Zhu, Y.L.; Huang, L.; Zeng, Z.Y.; Wan, H.J.; Li, Y.W. Study on Cu–Mn–Si catalysts for synthesis of cyclohexanone and 2-methylfuran through the coupling process. *Catal. Commun.* **2008**, *9*, 342–348.
52. Limacher, A.; Kerler, J.; Davidek, T.; Schmalzried, F.; Blank, I. Formation of furan and methylfuran by Maillard-type reactions in model systems and food. *J. Agric. Food Chem.* **2008**, *56*, 3639–3647.
53. Iqbal, S.; Liu, X.; Aldosari, O.F.; Miedziak, P.J.; Edwards, J.K.; Brett, G.L.; Akram, A.; King, G.M.; Davies, T.E.; Morgan, D.J.; et al. Conversion of furfuryl alcohol into 2-methylfuran at room temperature using Pd/TiO_2 catalyst. *Catal. Sci. Technol.* **2014**, *4*, 2280–2286.
54. Cui, J.; Tan, J.; Cui, X.; Zhu, Y.; Deng, T.; Ding, G.; Li, Y. Conversion of Xylose to Furfuryl Alcohol and 2-Methylfuran in a Continuous Fixed-Bed Reactor. *ChemSusChem* **2016**, *9*, 1259–1262.
55. Vorotnikov, V.; Mpourmpakis, G.; Vlachos, D.G. DFT study of furfural conversion to furan, furfuryl alcohol, and 2-methylfuran on Pd (111). *ACS Catal.* **2012**, *2*, 2496–2504.
56. Simmie, J.M.; Würmel, J. Harmonising Production, Properties and Environmental Consequences of Liquid Transport Fuels from Biomass—2,5-Dimethylfuran as a Case Study. *ChemSusChem* **2013**, *6*, 36–41.
57. Hu, L.; Lin, L.; Liu, S. Chemoselective hydrogenation of biomass-derived 5-hydroxymethylfurfural into the liquid biofuel 2,5-dimethylfuran. *Ind. Eng. Chem. Res.* **2014**, *53*, 9969–9978.
58. Qian, Y.; Zhu, L.; Wang, Y.; Lu, X. Recent progress in the development of biofuel 2,5-dimethylfuran. *Renew. Sustain. Energy Rev.* **2015**, *41*, 633–646.
59. Saha, B.; Abu-Omar, M.M. Current Technologies, Economics, and Perspectives for 2,5-Dimethylfuran Production from Biomass-Derived Intermediates. *ChemSusChem* **2015**, *8*, 1133–1142.
60. Xu, H.; Wang, C. A Comprehensive Review of 2,5-Dimethylfuran as a Biofuel Candidate. In *Biofuels from Lignocellulosic Biomass*; Wiley-VCH Verlag GmbH & Co. KGaA: Weinheim, Germany, 2016; pp. 105–129.
61. Hu, E.; Hu, X.; Wang, X.; Xu, Y.; Dearn, K.D.; Xu, H. On the fundamental lubricity of 2,5-dimethylfuran as a synthetic engine fuel. *Tribol. Int.* **2012**, *55*, 119–125.
62. Paine, J.B., III; Pithawalla, Y.B.; Naworal, J.D. Carbohydrate pyrolysis mechanisms from isotopic labeling: Part 4. The pyrolysis of d-glucose: The formation of furans. *J. Anal. Appl. Pyrolysis* **2008**, *83*, 37–63.
63. Binder, J.B.; Raines, R.T. Simple chemical transformation of lignocellulosic biomass into furans for fuels and chemicals. *J. Am. Chem. Soc.* **2009**, *131*, 1979–1985.
64. Thananatthanachon, T.; Rauchfuss, T.B. Efficient Production of the Liquid Fuel 2,5-Dimethylfuran from Fructose Using Formic Acid as a Reagent. *Angew. Chem. Int. Ed. Engl.* **2010**, *122*, 6766–6768.
65. Luijkx, G.C.; Huck, N.P.; van Rantwijk, F.; Maat, L.; van Bekkum, H. Ether formation in the hydrogenolysis of hydroxymethylfurfural over palladium catalysts in alcoholic solution. *Heterocycles* **2009**, *77*, 1037–1044.
66. Cai, H.; Li, C.; Wang, A.; Zhang, T. Biomass into chemicals: One-pot production of furan-based diols from carbohydrates via tandem reactions. *Catal. Today* **2014**, *234*, 59–65.
67. De, S.; Dutta, S.; Saha, B. One-pot conversions of lignocellulosic and algal biomass into liquid fuels. *ChemSusChem* **2012**, *5*, 1826–1833.
68. Jae, J.; Zheng, W.; Lobo, R.F.; Vlachos, D.G. Production of dimethylfuran from hydroxymethylfurfural through catalytic transfer hydrogenation with ruthenium supported on carbon. *ChemSusChem* **2013**, *6*, 1158–1162.
69. Jae, J.; Zheng, W.; Karim, A.M.; Guo, W.; Lobo, R.F.; Vlachos, D.G. The Role of Ru and RuO_2 in the Catalytic Transfer Hydrogenation of 5-Hydroxymethylfurfural for the Production of 2,5-Dimethylfuran. *ChemCatChem* **2014**, *6*, 848–856.
70. Hu, L.; Tang, X.; Xu, J.; Wu, Z.; Lin, L.; Liu, S. Selective transformation of 5-hydroxymethylfurfural into the liquid fuel 2,5-dimethylfuran over carbon-supported ruthenium. *Ind. Eng. Chem. Res.* **2014**, *53*, 3056–3064.
71. Huang, Y.B.; Chen, M.Y.; Yan, L.; Guo, Q.X.; Fu, Y. Nickel-Tungsten Carbide Catalysts for the Production of 2,5-Dimethylfuran from Biomass-Derived Molecules. *ChemSusChem* **2014**, *7*, 1068–1072.
72. Saha, B.; Bohn, C.M.; Abu-Omar, M.M. Zinc-Assisted Hydrodeoxygenation of Biomass-Derived 5-Hydroxymethylfurfural to 2,5-Dimethylfuran. *ChemSusChem* **2014**, *7*, 3095–3101.
73. Nishimura, S.; Ikeda, N.; Ebitani, K. Selective hydrogenation of biomass-derived 5-hydroxymethylfurfural (HMF) to 2,5-dimethylfuran (DMF) under atmospheric hydrogen pressure over carbon supported PdAu bimetallic catalyst. *Catal. Today* **2014**, *232*, 89–98.
74. Zu, Y.; Yang, P.; Wang, J.; Liu, X.; Ren, J.; Lu, G.; Wang, Y. Efficient production of the liquid fuel 2,5-dimethylfuran from 5-hydroxymethylfurfural over Ru/Co_3O_4 catalyst. *Appl. Catal. B Environ.* **2014**, *146*, 244–248.

75. Nagpure, A.S.; Venugopal, A.K.; Lucas, N.; Manikandan, M.; Thirumalaiswamy, R.; Chilukuri, S. Renewable fuels from biomass-derived compounds: Ru-containing hydrotalcites as catalysts for conversion of HMF to 2,5-dimethylfuran. *Catal. Sci. Technol.* **2015**, *5*, 1463–1472.
76. Upare, P.P.; Hwang, D.W.; Hwang, Y.K.; Lee, U.H.; Hong, D.Y.; Chang, J.S. An integrated process for the production of 2,5-dimethylfuran from fructose. *Green Chem.* **2015**, *17*, 3310–3313.
77. Yang, P.; Cui, Q.; Zu, Y.; Liu, X.; Lu, G.; Wang, Y. Catalytic production of 2,5-dimethylfuran from 5-hydroxymethylfurfural over Ni/Co_3O_4 catalyst. *Catal. Commun.* **2015**, *66*, 55–59.
78. Gawade, A.B.; Tiwari, M.S.; Yadav, G.D. Biobased Green Process: Selective Hydrogenation of 5-Hydroxymethylfurfural to 2,5-Dimethyl Furan under Mild Conditions Using Pd-Cs2. 5H0. 5PW12O40/K-10 Clay. *ACS Sustain. Chem. Eng.* **2016**, *4*, 4113–4123.
79. Shi, J.; Wang, Y.; Yu, X.; Du, W.; Hou, Z. Production of 2,5-dimethylfuran from 5-hydroxymethylfurfural over reduced graphene oxides supported Pt catalyst under mild conditions. *Fuel* **2016**, *163*, 74–79.
80. Chen, B.; Li, F.; Huang, Z.; Yuan, G. Carbon-coated Cu-Co bimetallic nanoparticles as selective and recyclable catalysts for production of biofuel 2,5-dimethylfuran. *Appl. Catal. B Environ.* **2017**, *200*, 192–199.
81. Dutta, S.; Mascal, M. Novel Pathways to 2,5-Dimethylfuran via Biomass-Derived 5-(Chloromethyl) furfural. *ChemSusChem* **2014**, *7*, 3028–3030.
82. Kazi, F.K.; Patel, A.D.; Serrano-Ruiz, J.C.; Dumesic, J.A.; Anex, R.P. Techno-economic analysis of dimethylfuran (DMF) and hydroxymethylfurfural (HMF) production from pure fructose in catalytic processes. *Chem. Eng. J.* **2011**, *169*, 329–338.
83. Smith, M.D.; Mostofian, B.; Cheng, X.; Petridis, L.; Cai, C.M.; Wyman, C.E.; Smith, J.C. Cosolvent pretreatment in cellulosic biofuel production: Effect of tetrahydrofuran-water on lignin structure and dynamics. *Green Chem.* **2016**, *18*, 1268–1277.
84. Wilson, C.L. 16. Reactions of furan compounds. Part III. Formation of tetrahydrofuran, 2,3-dihydrofuran, and other substances by passage of tetrahydrofurfuryl alcohol vapour over a nickel catalyst. *J. Chem. Soc.* **1945**, 52–57, doi:10.1039/JR9450000052.
85. Bagnall, W.H.; Goodings, E.P.; Wilson, C.L. Reactions of Furan Compounds. XII. Elimination of the Side Chain of Tetrahydrofurfuryl Alcohol Using Nickel-Copper Catalysts1. *J. Am. Chem. Soc.* **1951**, *73*, 4794–4798.
86. Kanetaka, J.; Asano, T.; Masamune, S. New process for production of tetrahydrofuran. *Ind. Eng. Chem.* **1970**, *62*, 24–32.
87. Luque, R.; Clark, J.H.; Yoshida, K.; Gai, P.L. Efficient aqueous hydrogenation of biomass platform molecules using supported metal nanoparticles on Starbons®. *Chem. Commun.* **2009**, *35*, 5305–5307.
88. Minh, D.P.; Besson, M.; Pinel, C.; Fuertes, P.; Petitjean, C. Aqueous-phase hydrogenation of biomass-based succinic acid to 1, 4-butanediol over supported bimetallic catalysts. *Top. Catal.* **2010**, *53*, 1270–1273.
89. Hong, U.G.; Park, H.W.; Lee, J.; Hwang, S.; Yi, J.; Song, I.K. Hydrogenation of succinic acid to tetrahydrofuran (THF) over rhenium catalyst supported on H_2SO_4-treated mesoporous carbon. *Appl. Catal. A Gen.* **2012**, *415*, 141–148.
90. Zeitsch, K.J. *The Chemistry and Technology of Furfural and Its Many by-Products*; Elsevier: Amsterdam, The Netherlands, 2000; Volume 13.
91. Yan, K.; Wu, G.; Lafleur, T.; Jarvis, C. Production, properties and catalytic hydrogenation of furfural to fuel additives and value-added chemicals. *Renew. Sustain. Energy Rev.* **2014**, *38*, 663–676.
92. Godawa, C.; Gaset, A.; Kalck, P.; Maire, Y. Mise en oeuvre d'un catalyseur actif pour l'hydrogenation selective du furanne en tetrahydrofuranne. *J. Mol. Catal.* **1986**, *34*, 199–212.
93. Godawa, C.; Rigal, L.; Gaset, A. Palladium catalyzed hydrogenation of furan: Optimization of production conditions for tetrahydrofuran. *Resour. Conserv. Recycl.* **1990**, *3*, 201–216.
94. Corma, A.; Iborra, S.; Velty, A. Chemical routes for the transformation of biomass into chemicals. *Chem. Rev.* **2007**, *107*, 2411–2502.
95. Kremer, F.; Heuser, B.; Pischinger, S. Furanoids. In *Biofuels from Lignocellulosic Biomass*; Wiley-VCH Verlag GmbH & Co. KGaA: Weinheim, Germany, 2016; pp. 131–158.
96. Zhang, W.; Zhu, Y.; Niu, S.; Li, Y. A study of furfural decarbonylation on K-doped Pd/Al_2O_3 catalysts. *J. Mol. Catal. A Chem.* **2011**, *335*, 71–81.
97. Alonso, D.M.; Bond, J.Q.; Dumesic, J.A. Catalytic conversion of biomass to biofuels. *Green Chem.* **2010**, *12*, 1493–1513.

98. Christian, R.V., Jr.; Brown, H.D.; Hixon, R. Derivatives of γ-Valerolactone, 1,4-Pentanediol and 1,4-Di-(β-cyanoethoxy)-pentane1. *J. Am. Chem. Soc.* **1947**, *69*, 1961–1963.
99. Yan, K.; Liao, J.; Wu, X.; Xie, X. A noble-metal free Cu-catalyst derived from hydrotalcite for highly efficient hydrogenation of biomass-derived furfural and levulinic acid. *RSC Adv.* **2013**, *3*, 3853–3856.
100. Bozell, J.J.; Moens, L.; Elliott, D.; Wang, Y.; Neuenscwander, G.; Fitzpatrick, S.; Bilski, R.; Jarnefeld, J. Production of levulinic acid and use as a platform chemical for derived products. *Resour. Conserv. Recycl.* **2000**, *28*, 227–239.
101. Mehdi, H.; Fábos, V.; Tuba, R.; Bodor, A.; Mika, L.T.; Horváth, I.T. Integration of homogeneous and heterogeneous catalytic processes for a multi-step conversion of biomass: From sucrose to levulinic acid, γ-valerolactone, 1,4-pentanediol, 2-methyl-tetrahydrofuran, and alkanes. *Top. Catal.* **2008**, *48*, 49–54.
102. Du, X.L.; Bi, Q.Y.; Liu, Y.M.; Cao, Y.; He, H.Y.; Fan, K.N. Tunable copper-catalyzed chemoselective hydrogenolysis of biomass-derived γ-valerolactone into 1,4-pentanediol or 2-methyltetrahydrofuran. *Green Chem.* **2012**, *14*, 935–939.
103. Upare, P.P.; Lee, J.M.; Hwang, Y.K.; Hwang, D.W.; Lee, J.H.; Halligudi, S.B.; Hwang, J.S.; Chang, J.S. Direct hydrocyclization of biomass-derived levulinic acid to 2-methyltetrahydrofuran over nanocomposite copper/silica catalysts. *ChemSusChem* **2011**, *4*, 1749–1752.
104. Geilen, F.; Engendahl, B.; Harwardt, A.; Marquardt, W.; Klankermayer, J.; Leitner, W. Selective and flexible transformation of biomass-derived platform chemicals by a multifunctional catalytic system. *Angew. Chem. Int. Ed.* **2010**, *122*, 5642–5646.
105. Al-Shaal, M.G.; Dzierbinski, A.; Palkovits, R. Solvent-free γ-valerolactone hydrogenation to 2-methyltetrahydrofuran catalysed by Ru/C: A reaction network analysis. *Green Chem.* **2014**, *16*, 1358–1364.
106. Elliott, D.C.; Frye, J.G. Hydrogenated 5-Carbon Compound and Method of Making. U.S. Patent 5,883,266, 16 March 1999.
107. Huber, G.W.; Iborra, S.; Corma, A. Synthesis of transportation fuels from biomass: Chemistry, catalysts, and engineering. *Chem. Rev.* **2006**, *106*, 4044–4098.
108. Ahmed, I. Processes for the Preparation of 2-Methylfuran and 2-Methyltetrahydrofuran. U.S. Patent 6,479,677, 12 November 2002.
109. Yang, W.; Sen, A. One-Step Catalytic Transformation of Carbohydrates and Cellulosic Biomass to 2,5-Dimethyltetrahydrofuran for Liquid Fuels. *ChemSusChem* **2010**, *3*, 597–603.
110. Sen, A.; Yang, W. One-Step Catalytic Conversion of Biomass-Derived Carbohydrates to Liquid Fuels. U.S. Patent 0,307,050, 9 December 2010.
111. Liu, R.; Zhou, X.; Zhai, L. Theoretical investigation of unimolecular decomposition channels of furan4. *J. Comput. Chem.* **1998**, *19*, 240–249.
112. Liu, R.; Zhou, X.; Zuo, T. The pyrolysis mechanism of furan revisited. *Chem. Phys. Lett.* **2000**, *325*, 457–464.
113. Sendt, K.; Bacskay, G.B.; Mackie, J.C. Pyrolysis of furan: Ab initio quantum chemical and kinetic modeling studies. *J. Phys. Chem. A* **2000**, *104*, 1861–1875.
114. Lifshitz, A.; Bidani, M.; Bidani, S. Thermal reactions of cyclic ethers at high temperatures. III. Pyrolysis of furan behind reflected shocks. *J. Phys. Chem.* **1986**, *90*, 5373–5377.
115. Davis, A.C.; Sarathy, S.M. Computational Study of the Combustion and Atmospheric Decomposition of 2-Methylfuran. *J. Phys. Chem. A* **2013**, *117*, 7670–7685.
116. Somers, K.P.; Simmie, J.M.; Curran, H.; Metcalfe, W.K. The Pyrolysis of 2-Methylfuran: A Quantum Chemical, Statistical Rate Theory and Kinetic Modelling Study. *Phys. Chem. Chem. Phys.* **2014**, *16*, 5349–5367.
117. Hudzik, J.M.; Bozzelli, J.W. Thermochemistry of Hydroxyl and Hydroperoxide Substituted Furan, Methylfuran, and Methoxyfuran. *J. Phys. Chem. A* **2017**, *121*, 4523–4544.
118. Zhang, W.; Du, B.; Mu, L.; Feng, C. Mechanism for the gas-phase reaction between OH and 3-methylfuran: A theoretical study. *Int. J. Quantum Chem.* **2008**, *108*, 1232–1238.
119. Simmie, J.M.; Metcalfe, W.K. Ab initio study of the decomposition of 2,5-dimethylfuran. *J. Phys. Chem. A* **2011**, *115*, 8877–8888.
120. Sirjean, B.; Fournet, R. Theoretical study of the thermal decomposition of the 5-methyl-2-furanylmethyl radical. *J. Phys. Chem. A* **2012**, *116*, 6675–6684.
121. Friese, P.; Simmie, J.M.; Olzmann, M. The reaction of 2,5-dimethylfuran with hydrogen atoms—An experimental and theoretical study. *Proc. Combust. Inst.* **2013**, *34*, 233–239.

122. Sirjean, B.; Fournet, R. Theoretical study of the reaction 2,5-dimethylfuran+ H → products. *Proc. Combust. Inst.* **2013**, *34*, 241–249.
123. Ferraz-Santos, T.; Bauerfeldt, G. Ab Initio Study of the Reactions of OH Radical with 2,5-Dimethylfuran. In Proceedings of the European Combustion Meeting, Budapest, Hungary, 30 March–2 April 2015.
124. Simmie, J.M.; Curran, H.J. Formation Enthalpies and Bond Dissociation Energies of Alkylfurans. The Strongest C–X Bonds Known? *J. Phys. Chem. A* **2009**, *113*, 5128–5137.
125. Feller, D.; Simmie, J.M. High-level ab initio enthalpies of formation of 2,5-dimethylfuran, 2-methylfuran, and furan. *J. Phys. Chem. A* **2012**, *116*, 11768–11775.
126. Zhang, W.; Feng, C.; Du, B.; Mu, L. An ab initio and density functional theory study on the mechanism for the reaction of OH with 2-ethylfuran. *Struct. Chem.* **2009**, *20*, 525–532.
127. Smith, A.R.; Meloni, G. Absolute photoionization cross sections of furanic fuels: 2-ethylfuran, 2-acetylfuran and furfural. *J. Mass Spectrom.* **2015**, *50*, 1206–1213.
128. Zhou, C.W.; Simmie, J.M.; Somers, K.P.; Goldsmith, C.F.; Curran, H.J. Chemical Kinetics of Hydrogen Atom Abstraction from Allylic Sites by (3)O_2; Implications for Combustion Modeling and Simulation. *J. Phys. Chem. A* **2017**, *121*, 1890–1899.
129. Chakravarty, H.K.; Fernandes, R.X. Reaction kinetics of hydrogen abstraction reactions by hydroperoxyl radical from 2-methyltetrahydrofuran and 2,5-dimethyltetrahydrofuran. *J. Phys. Chem. A* **2013**, *117*, 5028–5041.
130. Parab, P.R.; Sakade, N.; Sakai, Y.; Fernandes, R.; Heufer, K.A. Theoretical investigation of intramolecular hydrogen shift reactions in 3-methyltetrahydrofuran (3-MTHF) oxidation. *J. Phys. Chem. A* **2015**, *119*, 10917–10928.
131. Parab, P.R.; Sakade, N.; Sakai, Y.; Fernandes, R.; Heufer, K.A. A Computational Kinetics Study on the Intramolecular Hydrogen Shift Reactions of Alkylperoxy Radicals in 2-Methyltetrahydrofuran Oxidation. *Int. J. Chem. Kinet.* **2017**, *49*, 419–437.
132. Antonov, I.O.; Zádor, J.; Rotavera, B.; Papajak, E.; Osborn, D.L.; Taatjes, C.A.; Sheps, L. Pressure-dependent competition among reaction pathways from first-and second-O_2 additions in the low-temperature oxidation of tetrahydrofuran. *J. Phys. Chem. A* **2016**, *120*, 6582–6595.
133. Badovskaya, L.; Povarova, L. Oxidation of furans. *Chem. Heterocycl. Compd.* **2009**, *45*, 1023–1034.
134. Grela, M.; Amorebieta, V.; Colussi, A. Very low pressure pyrolysis of furan, 2-methylfuran and 2,5-dimethylfuran. The stability of the furan ring. *J. Phys. Chem.* **1985**, *89*, 38–41.
135. Bruinsma, O.S.; Tromp, P.J.; de Sauvage Nolting, H.J.; Moulijn, J.A. Gas phase pyrolysis of coal-related aromatic compounds in a coiled tube flow reactor: 2. Heterocyclic compounds, their benzo and dibenzo derivatives. *Fuel* **1988**, *67*, 334–340.
136. Organ, P.P.; Mackie, J.C. Kinetics of pyrolysis of furan. *J. Chem. Soc. Faraday Trans.* **1991**, *87*, 815–823.
137. Fulle, D.; Dib, A.; Kiefer, J.; Zhang, Q.; Yao, J.; Kern, R. Pyrolysis of furan at low pressures: Vibrational relaxation, unimolecular dissociation, and incubation times. *J. Phys. Chem. A* **1998**, *102*, 7480–7486.
138. Urness, K.N. A Molecular Picture of Biofuel Decomposition: Pyrolysis of Furan and Select Furanics. Ph.D. Thesis, University of Colorado at Boulder, Boulder, CO, USA, 2014.
139. Cheng, Z.; Tan, Y.; Wei, L.; Xing, L.; Yang, J.; Zhang, L.; Guan, Y.; Yan, B.; Chen, G.; Leung, D.Y. Experimental and kinetic modeling studies of furan pyrolysis: Fuel decomposition and aromatic ring formation. *Fuel* **2017**, *206*, 239–247.
140. Lifshitz, A.; Tamburu, C.; Shashua, R. Decomposition of 2-methylfuran. Experimental and modeling study. *J. Phys. Chem. A* **1997**, *101*, 1018–1029.
141. Cheng, Z.; He, S.; Xing, L.; Wei, L.; Li, W.; Li, T.; Yan, B.; Ma, W.; Chen, G. Experimental and Kinetic Modeling Study of 2-Methylfuran Pyrolysis at Low and Atmospheric Pressures. *Energy Fuels* **2017**, *31*, 896–903.
142. Lifshitz, A.; Tamburu, C.; Shashua, R. Thermal decomposition of 2,5-dimethylfuran. Experimental results and computer modeling. *J. Phys. Chem. A* **1998**, *102*, 10655–10670.
143. Djokic, M.; Carstensen, H.H.; Van Geem, K.M.; Marin, G.B. The thermal decomposition of 2,5-dimethylfuran. *Proc. Combust. Inst.* **2013**, *34*, 251–258.
144. Alexandrino, K.; Millera, Á.; Bilbao, R.; Alzueta, M.U. Novel aspects in the pyrolysis and oxidation of 2,5-dimethylfuran. *Proc. Combust. Inst.* **2015**, *35*, 1717–1725.
145. Alexandrino, K.; Salvo, P.; Millera, Á.; Bilbao, R.; Alzueta, M.U. Influence of the Temperature and 2,5-Dimethylfuran Concentration on Its Sooting Tendency. *Combust. Sci. Technol.* **2016**, *188*, 651–666.

146. De Bruycker, R.; Tran, L.S.; Carstensen, H.H.; Glaude, P.A.; Monge, F.; Alzueta, M.U.; Battin-Leclerc, F.; Van Geem, K.M. Experimental and modeling study of the pyrolysis and combustion of 2-methyltetrahydrofuran. *Combust. Flame* **2017**, *176*, 409–428.
147. Elwardany, A.; Es-Sebbar, E.; Khaled, F.; Farooq, A. A chemical kinetic study of the reaction of hydroxyl with furans. *Fuel* **2016**, *166*, 245–252.
148. Kim, D.; El Gharamti, I.; Hantouche, M.; Elwardany, A.E.; Farooq, A.; Bisetti, F.; Knio, O. A hierarchical method for Bayesian inference of rate parameters from shock tube data: Application to the study of the reaction of hydroxyl with 2-methylfuran. *Combust. Flame* **2017**, *184*, 55–67.
149. Alexandrino, K.; Millera, Á.; Bilbao, R.; Alzueta, M.U. 2-methylfuran Oxidation in the Absence and Presence of NO. *Flow Turbul. Combust.* **2016**, *96*, 343–362.
150. Eble, J.; Bänsch, C.; Olzmann, M. Kinetic Investigation of the Reactions of 2,5-Dimethylfuran and 2-Methylfuran with Hydroxyl Radicals. In Proceedings of the European Combustion Meeting, Budapest, Hungary, 30 March–2 April 2015.
151. Yoshizawa, H.; Nagashima, H.; Murakami, Y.; Takahashi, K. Kinetic Studies on the Reactions of Atomic Oxygen with Furan, 2-Methylfuran, and 2,5-Dimethylfuran at Elevated Temperatures. *Chem. Lett.* **2017**, *46*, 1207–1210. doi:10.1246/cl.170467.
152. Vanhove, G.; Yu, Y.; Boumehdi, M.A.; Frottier, O.; Herbinet, O.; Glaude, P.A.; Battin-Leclerc, F. Experimental study of tetrahydrofuran oxidation and ignition in low-temperature conditions. *Energy Fuels* **2015**, *29*, 6118–6125.
153. Jiao, C.; Adams, S.; Garscadden, A. Ionization of 2,5-dimethylfuran by electron impact and resulting ion-parent molecule reactions. *J. Appl. Phys.* **2009**, *106*, 013306.
154. Wu, S.; Yang, H.; Hu, J.; Shen, D.; Zhang, H.; Xiao, R. Pyrolysis of furan and its derivatives at 1100 °C: PAH products and DFT study. *J. Anal. Appl. Pyrolysis* **2016**, *120*, 252–257.
155. Tran, L.S.; Wang, Z.; Carstensen, H.H.; Hemken, C.; Battin-Leclerc, F.; Kohse-Höinghaus, K. Comparative experimental and modeling study of the low-to moderate-temperature oxidation chemistry of 2,5-dimethylfuran, 2-methylfuran, and furan. *Combust. Flame* **2017**, *181*, 251–269.
156. Tran, L.S.; Sirjean, B.; Glaude, P.A.; Fournet, R.; Battin-Leclerc, F. Progress in detailed kinetic modeling of the combustion of oxygenated components of biofuels. *Energy* **2012**, *43*, 4–18.
157. Fenard, Y.; Boumehdi, M.; Vanhove, G. Experimental and kinetic modeling study of 2-methyltetrahydrofuran oxidation under engine-relevant conditions. *Combust. Flame* **2017**, *178*, 168–181.
158. Tran, L.S.; Verdicchio, M.; Monge, F.; Martin, R.C.; Bounaceur, R.; Sirjean, B.; Glaude, P.A.; Alzueta, M.U.; Battin-Leclerc, F. An experimental and modeling study of the combustion of tetrahydrofuran. *Combust. Flame* **2015**, *162*, 1899–1918.
159. Liu, D.; Togbé, C.; Tran, L.S.; Felsmann, D.; Oßwald, P.; Nau, P.; Koppmann, J.; Lackner, A.; Glaude, P.A.; Sirjean, B.; et al. Combustion chemistry and flame structure of furan group biofuels using molecular-beam mass spectrometry and gas chromatography—Part I: Furan. *Combust. Flame* **2014**, *161*, 748–765.
160. Tran, L.S.; Togbé, C.; Liu, D.; Felsmann, D.; Oßwald, P.; Glaude, P.A.; Fournet, R.; Sirjean, B.; Battin-Leclerc, F.; Kohse-Höinghaus, K. Combustion chemistry and flame structure of furan group biofuels using molecular-beam mass spectrometry and gas chromatography—Part II: 2-Methylfuran. *Combust. Flame* **2014**, *161*, 766–779.
161. Togbé, C.; Tran, L.S.; Liu, D.; Felsmann, D.; Oßwald, P.; Glaude, P.A.; Sirjean, B.; Fournet, R.; Battin-Leclerc, F.; Kohse-Höinghaus, K. Combustion chemistry and flame structure of furan group biofuels using molecular-beam mass spectrometry and gas chromatography—Part III: 2,5-Dimethylfuran. *Combust. Flame* **2014**, *161*, 780–797.
162. Mehl, M.; Herbinet, O.; Dirrenberger, P.; Bounaceur, R.; Glaude, P.A.; Battin-Leclerc, F.; Pitz, W.J. Experimental and modeling study of burning velocities for alkyl aromatic components relevant to diesel fuels. *Proc. Combust. Inst.* **2015**, *35*, 341–348.
163. Thewes, M.; Muether, M.; Pischinger, S.; Budde, M.; Brunn, A.; Sehr, A.; Adomeit, P.; Klankermayer, J. Analysis of the Impact of 2-Methylfuran on Mixture Formation and Combustion in a Direct-Injection Spark-Ignition Engine. *Energy Fuels* **2011**, *25*, 5549–5561.
164. Hoppe, F.; Burke, U.; Thewes, M.; Heufer, A.; Kremer, F.; Pischinger, S. Tailor-Made Fuels from Biomass: Potentials of 2-butanone and 2-methylfuran in direct injection spark ignition engines. *Fuel* **2016**, *167*, 106–117.

165. Hoppe, F.; Heuser, B.; Thewes, M.; Kremer, F.; Pischinger, S.; Dahmen, M.; Hechinger, M.; Marquardt, W. Tailor-made fuels for future engine concepts. *Int. J. Engine Res.* **2016**, *17*, 16–27.
166. Hoppe, F.; Thewes, M.; Kremer, F.; Pischinger, S. Tailor-made Fuels for Highly Boosted Gasoline Engines. *ATZextra Worldw.* **2016**, *21*, 32–37.
167. Wei, H.; Feng, D.; Shu, G.; Pan, M.; Guo, Y.; Gao, D.; Li, W. Experimental investigation on the combustion and emissions characteristics of 2-methylfuran gasoline blend fuel in spark-ignition engine. *Appl. Energy* **2014**, *132*, 317–324.
168. Wei, H.; Gao, D.; Zhou, L.; Feng, D.; Chen, C.; Pei, Z. Experimental analysis on spray development of 2-methylfuran-gasoline blends using multi-hole DI injector. *Fuel* **2016**, *164*, 245–253.
169. Sivasubramanian, H. Effect of Ignition Delay (ID) on performance, emission and combustion characteristics of 2-Methyl Furan-Unleaded gasoline blends in a MPFI SI engine. *Alex. Eng. J.* **2017**, doi:10.1016/j.aej.2016.12.014.
170. Wei, H.; Feng, D.; Pan, M.; Pan, J. *Effects of Multiple Parameters on Cyclic Variation of a SI Engine Fueled with 2-Methylfuran Gasoline Blends*; SAE Technical Paper; SAE International: Warrendale, PA, USA, 2017.
171. Xiao, H.; Zeng, P.; Li, Z.; Zhao, L.; Fu, X. Combustion performance and emissions of 2-methylfuran diesel blends in a diesel engine. *Fuel* **2016**, *175*, 157–163.
172. Daniel, R.; Tian, G.; Xu, H.; Wyszynski, M.L.; Wu, X.; Huang, Z. Effect of spark timing and load on a DISI engine fuelled with 2,5-dimethylfuran. *Fuel* **2011**, *90*, 449–458.
173. Daniel, R.; Wei, L.; Xu, H.; Wang, C.; Wyszynski, M.L.; Shuai, S. Speciation of Hydrocarbon and Carbonyl Emissions of 2,5-Dimethylfuran Combustion in a DISI Engine. *Energy Fuels* **2012**, *26*, 6661–6668.
174. Daniel, R.; Tian, G.; Xu, H.; Shuai, S. Ignition timing sensitivities of oxygenated biofuels compared to gasoline in a direct-injection SI engine. *Fuel* **2012**, *99*, 72–82.
175. Daniel, R.; Wang, C.; Xu, H.; Tian, G. Effects of combustion phasing, injection timing, relative air-fuel ratio and variable valve timing on SI engine performance and emissions using 2,5-dimethylfuran. *SAE Int. J. Fuels Lubr.* **2012**, *5*, 855–866.
176. Wang, C.; Xu, H.; Herreros, J.M.; Lattimore, T.; Shuai, S. Fuel effect on particulate matter composition and soot oxidation in a direct-injection spark ignition (DISI) engine. *Energy Fuels* **2014**, *28*, 2003–2012.
177. Tian, G.; Li, H.; Xu, H.; Li, Y.; Raj, S.M. Spray characteristics study of DMF using phase doppler particle analyzer. *SAE Int. J. Passeng. Cars Mech. Syst.* **2010**, *3*, 948–958.
178. Tian, G.; Xu, H.; Daniel, R.; Li, H.; Li, Y. Spray characteristics and engine adaptability of 2,5-dimethylfuran. *J. Automot. Saf. Energy* **2010**, *2*, 132–140.
179. Wu, X.; Daniel, R.; Tian, G.; Xu, H.; Huang, Z.; Richardson, D. Dual-injection: The flexible, bi-fuel concept for spark-ignition engines fuelled with various gasoline and biofuel blends. *Appl. Energy* **2011**, *88*, 2305–2314.
180. Shukla, M.K.; Singh, E.; Singh, N.; Singal, S. Prospects of 2,5-dimethylfuran as a fuel: Physico-chemical and engine performance characteristics evaluation. *J. Mater. Cycles Waste Manag.* **2015**, *17*, 459–464.
181. Chen, G.; Shen, Y.; Zhang, Q.; Yao, M.; Zheng, Z.; Liu, H. Experimental study on combustion and emission characteristics of a diesel engine fueled with 2,5-dimethylfuran-diesel, n-butanol-diesel and gasoline-diesel blends. *Energy* **2013**, *54*, 333–342.
182. Liu, H.; Xu, J.; Zheng, Z.; Li, S.; Yao, M. Effects of fuel properties on combustion and emissions under both conventional and low temperature combustion mode fueling 2,5-dimethylfuran/diesel blends. *Energy* **2013**, *62*, 215–223.
183. Liu, H.; Zheng, Z.; Yao, M. *Effects of Fuel Physical and Chemical Properties on Combustion and Emissions on Both Metal and Optical Diesel Engines and on a Partially Premixed Burner*; SAE Technical Paper; SAE International: Warrendale, PA, USA, 2015.
184. Zhang, Q.; Chen, G.; Zheng, Z.; Liu, H.; Xu, J.; Yao, M. Combustion and emissions of 2,5-dimethylfuran addition on a diesel engine with low temperature combustion. *Fuel* **2013**, *103*, 730–735.
185. Zhang, Q.; Yao, M.; Luo, J.; Chen, H.; Zhang, X. Diesel engine combustion and emissions of 2,5-dimethylfuran-diesel blends with 2-ethylhexyl nitrate addition. *Fuel* **2013**, *111*, 887–891.
186. Chen, G.; Di, L.; Zhang, Q.; Zheng, Z.; Zhang, W. Effects of 2,5-dimethylfuran fuel properties coupling with EGR (exhaust gas recirculation) on combustion and emission characteristics in common-rail diesel engines. *Energy* **2015**, *93*, 284–293.
187. Xiao, H.; Hou, B.; Zeng, P.; Jiang, A.; Hou, X.; Liu, J. Combustion and emission characteristics of diesel engine fueled with 2,5-dimethylfuran and diesel blends. *Fuel* **2017**, *192*, 53–59.

188. Xiao, H.; Zeng, P.; Zhao, L.; Li, Z.; Fu, X. An experimental study of the combusition and emission performances of 2,5-dimethylfuran diesel blends on a diesel engine. *Therm. Sci.* **2017**, *21*, 543–553.
189. Zheng, Z.; Wang, X.; Yue, L.; Liu, H.; Yao, M. Effects of six-carbon alcohols, ethers and ketones with chain or ring molecular structures on diesel low temperature combustion. *Energy Convers. Manag.* **2016**, *124*, 480–491.
190. Wei, M.; Li, S.; Liu, J.; Guo, G.; Sun, Z.; Xiao, H. Effects of injection timing on combustion and emissions in a diesel engine fueled with 2,5-dimethylfuran-diesel blends. *Fuel* **2017**, *192*, 208–217.
191. Wang, C.; Xu, H.; Daniel, R.; Ghafourian, A.; Herreros, J.M.; Shuai, S.; Ma, X. Combustion characteristics and emissions of 2-methylfuran compared to 2,5-dimethylfuran, gasoline and ethanol in a DISI engine. *Fuel* **2013**, *103*, 200–211.
192. Nasrullah, M.; Gopal, K.R. Effect of Tetra Hydro Furan on Performance and Emission Characteristics of Ci Engine Fuelled With Methyl Ester of Jatropha. *Int. J. Emerg. Technol. Adv. Eng.* **2014**, *4*, 251–257.
193. Boot, M.D.; Tian, M.; Hensen, E.J.; Sarathy, S.M. Impact of fuel molecular structure on auto-ignition behavior—Design rules for future high performance gasolines. *Prog. Energy Combust. Sci.* **2017**, *60*, 1–25.
194. Eldeeb, M.A. Characterization and Chemical Kinetic Analysis of the Ignition of Representative Conventional and Bio-Derived Fuels. Ph.D. Thesis, Syracuse University, Syracuse, NY, USA, 2015.
195. Bergthorson, J.M.; Thomson, M.J. A review of the combustion and emissions properties of advanced transportation biofuels and their impact on existing and future engines. *Renew. Sustain. Energy Rev.* **2015**, *42*, 1393–1417.
196. Dagaut, P.; McGuinness, M.; Simmie, J.; Cathonnet, M. The ignition and oxidation of tetrahydrofuran: Experiments and kinetic modeling. *Combust. Sci. Technol.* **1998**, *135*, 3–29.
197. Eldeeb, M.A.; Akih-Kumgeh, B. Investigation of ignition behavior of dimethyl and ethyl isomers of cycloalkanes and furans. In Proceedings of the 25th International Colloquium on the Dynamics of Explosions and Reactive Systems (ICDERS), Leeds, UK, 2–7 August 2015.
198. Xu, N.; Tang, C.; Meng, X.; Fan, X.; Tian, Z.; Huang, Z. Experimental and kinetic study on the ignition delay times of 2,5-dimethylfuran and the comparison to 2-methylfuran and furan. *Energy Fuels* **2015**, *29*, 5372–5381.
199. Xu, N.; Wu, Y.; Tang, C.; Zhang, P.; He, X.; Wang, Z.; Huang, Z. Experimental study of 2,5-dimethylfuran and 2-methylfuran in a rapid compression machine: Comparison of the ignition delay times and reactivity at low to intermediate temperature. *Combust. Flame* **2016**, *168*, 216–227.
200. Xu, N.; Wu, Y.; Tang, C.; Zhang, P.; He, X.; Wang, Z.; Huang, Z. Ignition delay times of low alkylfurans at high pressures using a rapid compression machine. *Proc. Combust. Inst.* **2017**, *36*, 323–332.
201. Shen, H.P.S.; Oehlschlaeger, M.A. The autoignition of C_8H_{10} aromatics at moderate temperatures and elevated pressures. *Combust. Flame* **2009**, *156*, 1053–1062.
202. Wang, J.; Wang, X.; Fan, X.; Yang, K. *Shock Tube Experimental and Modeling Study of MTHF Ignition Characteristics at High Temperatures*; SAE Technical Paper; SAE International: Warrendale, PA, USA, 2015.
203. Wang, J.; Wang, X.; Fan, X.; Yang, K.; Zhang, Y. An ignition delay time and kinetic study of 2-methyltetrahydrofuran at high temperatures. *Fuel* **2016**, *186*, 758–769.
204. Sudholt, A.; Lee, C.; Klankermayer, J.; Fernandes, R.X.; Pitsch, H. Ignition characteristics of saturated and unsaturated furans. *Combust. Flame* **2016**, *171*, 133–136.
205. Fan, X.; Wang, X.; Wang, J.; Yang, K. Comparative Shock Tube and Kinetic Study on High-Temperature Ignition of 2,3-Dihydrofuran and 2,5-Dihydrofuran. *Energy Fuels* **2016**, *30*, 8727–8736.
206. Fan, X.; Wang, X.; Yang, K.; Li, Y.; Wu, C.; Li, Z. Experimental and Modeling Study on Ignition Characteristics of 2,5-Dihydrofuran. *SAE Int. J. Fuels Lubr.* **2016**, *9*, 315–321.
207. Tanaka, K.; Isobe, N.; Sato, K.; Okada, R.; Okada, H.; Fujisawa, Y.; Konno, M. Ignition Characteristics of 2,5-Dimethylfuran Compared with Gasoline and Ethanol. *SAE Int. J. Engines* **2015**, *9*, 39–46.
208. Nilsson, E.J.K.; Konnov, A.A. Flame Studies of Oxygenates. In *Cleaner Combustion: Developing Detailed Chemical Kinetic Models*; Battin-Leclerc, F., Simmie, J.M., Blurock, E., Eds.; Springer: London, UK, 2013; pp. 231–280.
209. Cheng, Z.; Niu, Q.; Wang, Z.; Jin, H.; Chen, G.; Yao, M.; Wei, L. Experimental and kinetic modeling studies of low-pressure premixed laminar 2-methylfuran flames. *Proc. Combust. Inst.* **2017**, *36*, 1295–1302.
210. Ma, X.; Xu, H.; Jiang, C.; Shuai, S. Ultra-high speed imaging and OH-LIF study of {DMF} and {MF} combustion in a {DISI} optical engine. *Appl. Energy* **2014**, *122*, 247–260.

211. Tao, K.; Gao, D.; Pei, Z. Impact of Initial Pressure and Mix Proportion on Flame Propagation Development in Premixed Combustion of 2-Methyl Furan Gasoline Mixed Fuel in Constant Volume Napalm Bomb. *J. Comput. Theor. Nanosci.* **2016**, *13*, 9373–9379.
212. Wu, X.; Huang, Z.; Yuan, T.; Zhang, K.; Wei, L. Identification of combustion intermediates in a low-pressure premixed laminar 2,5-dimethylfuran/oxygen/argon flame with tunable synchrotron photoionization. *Combust. Flame* **2009**, *156*, 1365–1376.
213. Wu, X.; Huang, Z.; Jin, C.; Wang, X.; Zheng, B.; Zhang, Y.; Wei, L. Measurements of laminar burning velocities and Markstein lengths of 2,5-dimethylfuran-air-diluent premixed flames. *Energy Fuels* **2009**, *23*, 4355–4362.
214. Wu, X.; Huang, Z.; Wang, X.; Jin, C.; Tang, C.; Wei, L.; Law, C.K. Laminar burning velocities and flame instabilities of 2,5-dimethylfuran–air mixtures at elevated pressures. *Combust. Flame* **2011**, *158*, 539–546.
215. Wu, X.; Huang, Z.; Jin, C.; Wang, X.; Wei, L. Laminar burning velocities and Markstein lengths of 2,5-dimethylfuran-air premixed flames at elevated temperatures. *Combust. Sci. Technol.* **2011**, *183*, 220–237.
216. Tian, G.; Daniel, R.; Li, H.; Xu, H.; Shuai, S.; Richards, P. Laminar Burning Velocities of 2,5-Dimethylfuran Compared with Ethanol and Gasoline. *Energy Fuels* **2010**, *24*, 3898–3905.
217. Wei, L.; Tong, L.; Xu, J.; Wang, Z.; Jin, H.; Yao, M.; Zheng, Z.; Li, H.; Xu, H. Primary combustion intermediates in low-pressure premixed laminar 2,5-dimethylfuran/oxygen/argon flames. *Combust. Sci. Technol.* **2014**, *186*, 355–376.
218. Liu, X.; Yao, M.; Wang, Y.; Wang, Z.; Jin, H.; Wei, L. Experimental and kinetic modeling study of a rich and a stoichiometric low-pressure premixed laminar 2,5-dimethylfuran/oxygen/argon flames. *Combust. Flame* **2015**, *162*, 4586–4597.
219. Gogoi, B.; Raj, A.; Alrefaai, M.M.; Stephen, S.; Anjana, T.; Pillai, V.; Bojanampati, S. Effects of 2,5-dimethylfuran addition to diesel on soot nanostructures and reactivity. *Fuel* **2015**, *159*, 766–775.
220. Russo, C.; D'Anna, A.; Ciajolo, A.; Sirignano, M. Analysis of the chemical features of particles generated from ethylene and ethylene/2,5 dimethyl furan flames. *Combust. Flame* **2016**, *167*, 268–273.
221. Li, Q.; Fu, J.; Wu, X.; Tang, C.; Huang, Z. Laminar flame speeds of DMF/iso-octane-air-N_2/CO_2 mixtures. *Energy Fuels* **2012**, *26*, 917–925.
222. Wu, X.; Li, Q.; Fu, J.; Tang, C.; Huang, Z.; Daniel, R.; Tian, G.; Xu, H. Laminar burning characteristics of 2,5-dimethylfuran and iso-octane blend at elevated temperatures and pressures. *Fuel* **2012**, *95*, 234–240.
223. Jiang, Y.; Xu, H.; Ma, X.; Bao, X.; Wang, B. Laminar burning characteristics of 2-MTHF compared with ethanol and isooctane. *Fuel* **2017**, *190*, 10–20.
224. Ma, X.; Jiang, C.; Xu, H.; Shuai, S.; Ding, H. Laminar Burning Characteristics of 2-Methylfuran Compared with 2,5-Dimethylfuran and Isooctane. *Energy Fuels* **2013**, *27*, 6212–6221.
225. Gillespie, F.R. An Experimental and Modelling Study of the Combustion of Oxygenated Hydrocarbons. Ph.D. Thesis, NUI Galway, Galway, Ireland, 2014.
226. Tran, L.S.; Sirjean, B.; Glaude, P.A.; Kohse-Höinghaus, K.; Battin-Leclerc, F. Influence of substituted furans on the formation of Polycyclic Aromatic Hydrocarbons in flames. *Proc. Combust. Inst.* **2015**, *35*, 1735–1743.
227. Sirignano, M.; Conturso, M.; D'Anna, A. Effect of furans on particle formation in diffusion flames: An experimental and modeling study. *Proc. Combust. Inst.* **2015**, *35*, 525–532.
228. Conturso, M.; Sirignano, M.; D'Anna, A. Effect of furanic biofuels on particles formation in premixed ethylene-air flames: An experimental study. *Fuel* **2016**, *175*, 137–145.
229. Saggese, C.; Cuoci, A.; Frassoldati, A.; Faravelli, T.; Ranzi, E. Gas Phase Kinetics of Volatiles from Biomass Pyrolysis. Note II: Furan, 2-methyl-furan, and 2,5-dimethylfuran. In Proceedings of the 36th Meeting of the Italian Section of the Combustion Institute, Procida, Italy, 13–15 June 2013.
230. Metcalfe, W.K.; Burke, S.M.; Ahmed, S.S.; Curran, H.J. A hierarchical and comparative kinetic modeling study of C1–C2 hydrocarbon and oxygenated fuels. *Int. J. Chem. Kinet.* **2013**, *45*, 638–675.
231. Sirignano, M.; Kent, J.; D'Anna, A. Modeling formation and oxidation of soot in nonpremixed flames. *Energy Fuels* **2013**, *27*, 2303–2315.
232. Sirignano, M.; Kent, J.; D'Anna, A. Detailed modeling of size distribution functions and hydrogen content in combustion-formed particles. *Combust. Flame* **2010**, *157*, 1211–1219.
233. D'Anna, A.; Sirignano, M.; Kent, J. A model of particle nucleation in premixed ethylene flames. *Combust. Flame* **2010**, *157*, 2106–2115.

234. Curran, H.J.; Gaffuri, P.; Pitz, W.; Westbrook, C. A comprehensive modeling study of iso-octane oxidation. *Combust. Flame* **2002**, *129*, 253–280.
235. Mehl, M.; Pitz, W.J.; Westbrook, C.K.; Curran, H.J. Kinetic modeling of gasoline surrogate components and mixtures under engine conditions. *Proc. Combust. Inst.* **2011**, *33*, 193–200.